Phylogenetics and biochemistry elucidate the evolutionary link between l-malate and l-lactate dehydrogenases and disclose an intermediate group of sequences with mix functional properties

Céline Brochier-Armanet, Dominique Madern

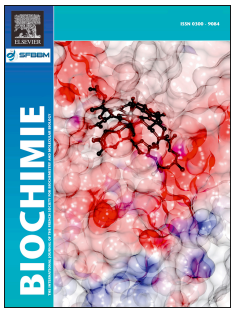

Phylogenetics and biochemistry elucidate the evolutionary link between L-malate and L-lactate dehydrogenases and disclose an intermediate group of sequences with mix functional properties

Céline Brochier-Armanet, Dominique Madern

PII: S0300-9084(21)00196-6

DOI: https://doi.org/10.1016/j.biochi.2021.08.004

Reference: BIOCHI 6175

To appear in: *Biochimie*

Received Date: 17 April 2021

Revised Date: 19 July 2021

Accepted Date: 15 August 2021

Please cite this article as: Cé. Brochier-Armanet, D. Madern, Phylogenetics and biochemistry elucidate the evolutionary link between L-malate and L-lactate dehydrogenases and disclose an intermediate group of sequences with mix functional properties, *Biochimie* (2021), doi: https://doi.org/10.1016/j.biochi.2021.08.004.

Phylogenetics and biochemistry elucidate the evolutionary link between L-malate and L-lactate dehydrogenases and disclose an intermediate group of sequences with mix functional properties

Céline-Brochier-Armanet[1,*] and Dominique Madern[2,*]

Affiliations.

1. Université de Lyon, Université Lyon 1, CNRS, Laboratoire de Biométrie et Biologie Évolutive UMR 5558, F-69622 Villeurbanne, France.
2. Univ. Grenoble Alpes, CEA, CNRS, IBS, 38000 Grenoble, France
* Corresponding authors

Abstract.

The NAD(P)-dependent malate dehydrogenases (MDH) (EC 1.1.1.37) and NAD-dependent lactate dehydrogenases (LDH) (EC. 1.1.1.27) form a large super-family that has been characterized in organisms belonging to the three Domains of Life. MDH catalyses the reversible conversion of the oxaloacetate into malate, while LDH operates at the late stage of glycolysis by converting pyruvate into lactate. Phylogenetic studies proposed that the LDH / MDH superfamily encompasses five main groups of enzymes. Here, starting from 16,052 reference proteomes, we reinvestigated the relationship between MDH and LDH. We showed that the LDH / MDH superfamily encompasses three main families: MDH1, MDH2, and a large family encompassing MDH3, LDH, and L-2-hydroxyisocaproate dehydrogenases (HicDH) sequences. An in-depth analysis of the phylogeny of the MDH3 / LDH / HicDH family and of the nature of three important amino acids located within the catalytic site and involved in binding and substrate discrimination, revealed a large group of sequences displaying unexpected combinations of amino acids at these three critical positions. This group branched in-between MDH3 and LDH sequences. The functional characterization of several enzymes from this intermediate group disclosed a mix of functional properties, indicating that the MDH3 / LDH / HicDH family is much more diverse than previously thought, and blurred the frontier between MDH3 and LDH enzymes. Present-days enzymes of the intermediate group are a valuable material to study the evolutionary steps that led to functional diversity and emergence of allosteric regulation within the LDH / MDH superfamily.

Keywords.

Malate dehydrogenase, lactate dehydrogenase, molecular evolution, allosteric regulation, *Archaea*, neofunctionalization.

Declarations of interest: none

Author Agreement: all authors have seen and approved the final version of the manuscript being submitted.

Abbreviations

aLRT: approximate likelihood ratio test
BV: Bootstrap value
FBP: fructose 1,6-bisphosphate
HGT: Horizontal gene transfer
HMM: Hidden Markov Model
LDH: L-Lactate dehydrogenases
LG model: Le and Gascuel model
MDH: Malate dehydrogenase
ML: Maximum Likelihood
NADH: nicotinamide adenine dinucleotide
NADPH: nicotinamide adenine dinucleotide phosphate
OAA: oxaloacetate
PYR: pyruvate
PVC superphylum: *Planctomycetes-Verrucomicrobia-Chlamydiae* superphylum
SH: Shimodaira-Hasegawa

Highlights

Phylogenetic analyses disentangle the relationships between malate dehydrogenases and lactate dehydrogenases.

The study reveals an intermediate group of enzymes that reflects an early and step-wise functional divergence between malate dehydrogenases and lactate dehydrogenases.

Neofunctionalization and subfunctionalization contribute to evolution of malate dehydrogenases and lactate dehydrogenases.

The work suggests that present-day enzymes such as in *Tolumonas auensis* are descendant of an ancient group of enzymes in which allostery evolved.

1. Introduction.

Central metabolism is a key chemical process that provides energy and biochemical precursors for growing and multiplication of cells. Even if the total metabolic capacity is mostly similar in *Archaea* and *Bacteria*, variations are observed across lineages and even at the strain level [1-3]. These variations reflect the diversity of species, lifestyles, and adaptations to different environments. Understanding functions and roles of enzymes involved in metabolism is not only of academic importance but also of a medical interest. For instance, in human, metabolic diseases are responsible of cancer and the selective inhibition of metabolic enzymes that favour growing of tumour cells in tumour microenvironments is a promising therapeutic strategy [4-6]. Amongst these enzymes, L-lactate dehydrogenases (LDH, EC 1.1.1.27) are one of the main targets for the development of such inhibitors [7].

LDH are cytosolic tetrameric enzymes involved in the anaerobic metabolism of glucose when oxygen is absent or in limited supply. They reversibly transform pyruvate (PYR) into lactate using NADH as coenzyme (see [8] and references therein). LDHs are found in eukaryotes and bacteria [9] and can be distinguished by their capacity to regulate (or not) their activity owing allosteric control. Most of the bacterial LDH display sigmoidal kinetics for pyruvate (homotropic activation) and are allosterically activated by fructose 1,6-bisphosphate (FBP) (heterotropic activation) [9, 10]. According to chemical similarities regarding substrate and catalytic mechanism, a connection between LDH and malate dehydrogenases (MDH, EC 1.1.1.37) was established [11]. Indeed, both enzymes catalyse the reversible conversion of 2-hydroxyacids to the corresponding 2-ketoacids. In bacteria, MDH is involved in the tricarboxylicacid cycle (TCA) and oxidize oxaloacetate (OAA) into malate using either NADH or NADPH as coenzyme. In eukaryotes, several forms of MDH coexist, with distinct enzymes being associated to specific cell compartments. For example, in human, the mitochondrial enzyme operates in the TCA cycle, whereas the cytosolic MDH is connected to membrane transporters and contributes to balance the redox state of cells via the indirect transfer of reducing equivalents between the cytosol and the mitochondria [12]. In Plantae and in Fungi, additional MDH are present in peroxisomes and chloroplasts [13-15].

The hypothesis of an evolutionary link between LDH and MDH has been reinforced when the first crystallographic structures have been resolved [16]. At that time, MDH were classified into two main groups of dimeric enzymes (hereafter referred as MDH1 and MDH2) [17, 18]. MDH1 contains eukaryotic cytosolic and various bacterial enzymes, while MDH2 encompasses eukaryotic glyoxysomal and mitochondrial enzymes and some bacterial proteins [17]. Later, a third group of MDH (hereafter referred as MDH3 also frequently mentioned as LDH-like MDH) has been described (see [17] and references therein). At the sequence level, MDH3 are more similar to LDH, suggesting a closer evolutionary link [17].

Consistently, it has been shown that the MDH3 of the crenarchaeon *Ignicoccus islandicus* that recognizes OAA as main substrate has a low activity using PYR [19]. While MDH1 and MDH2 are dimeric, MDH3 display an LDH-like tetrameric organisation. However, some dimeric MDH3 exist as exemplified by the enzyme from Archaeoglobus fulgidus [20]. MDH3 are mainly found in bacteria, in some archaea, but not in eukaryotes, to the exception of apicomplexan [21, 22]. Recently, L-2-hydroxyisocaproate dehydrogenases (hereafter referred as to HicDH) have been described and are phylogenetically related to LDH and MDH3 [17, 22]. HicDH are tetrameric NADH-dependent oxidoreductases that catalyse the stereospecific oxidation of aliphatic branched *(S)*-2-hydroxycaboxylic acids [23].

Twenty years ago, an evolutionary scenario describing the functional divergence between LDH and MDH proposed that an ancient gene duplication of an MDH gene of unknown oligomeric state led to the group of tetrameric MDH (i.e. MDH3) and to the group of dimeric MDH, that evolved later toward MDH1 and MDH2. This ancient duplication event did not impact the function of the resulting paralogues, i.e. the production of malate from OAA. The scenario proposed also that a duplication of the tetrameric MDH3 occurred. One of the two resulting paralogues conserved the ancestral functionality (i.e. the use of OAA as substrate), whereas the second paralogue evolved toward canonical LDH [17]. The hypothesis that LDH derive from MDH was reinforced by recent studies showing that the LDH enzymes of *Plasmodium*-related species and of *Cryptosporidium* derived independently from ancient MDHs [21, 22, 24]. ~~Noticed that~~ Noticeably a single case of LDH evolution from cytosolic dimeric MDH1 has been reported in *Trichomonas vaginalis* [25, 26]. Altogether, four independent functional shifts from MDH to LDH activity have been documented [17, 22, 25].
Since these early studies, the number of sequences belonging to the LDH / MDH superfamily has dramatically increased (up to 56,000 according to InterPro), providing a valuable material to reinvestigate the evolutionary history of this superfamily. Concomitantly, comparative biochemical investigations of both wild-type LDH and MDH enzymes, and site-directed mutagenesis experiments have produced a large body of kinetics and ligand-binding information [19, 22, 27-36]. When analysed in light of crystallographic structures, this data allows to describe the catalytic mechanisms of LDH and MDH (summarized in Supplementary Figure S1). The chemical reaction proceeds by transferring a hydride ion from their coenzyme to the C2 carbon of their respective substrates (i.e. PYR or OAA, respectively). The universally conserved R171 of LDH and MDH coordinates the carboxylate moiety of PYR and OAA. For the sake of clarity, residues numbering is accordingly to the normalized structural numbering based on LDH structure of *Squalus ancathias* (PDB code 1LDM) [37]. All these studies also revealed the major role of three amino acid residues with

respect to the discrimination between PYR and OAA. These three residues are located within the catalytic vacuole of LDH and MDH at positions 102, 199, and 246.

The selection between PYR and OAA is mostly due to the nature of amino acid at position 102. In MDH, the arginine at this position helps to anchor the second carboxylate extremity of OAA, while in LDH, glutamine, a polar residue, accommodates the uncharged extremity of PYR. The amino acid at position 246 also contributes to discriminate between the two substrates. In MDH, the small lateral chain of A246 accommodates the methylene carboxylate group of OAA [32], while in LDH, the larger side chain of T246 is considered as unfavourable for OAA-binding because of stearic hindrance [27]. In LDH and MDH, charge neutrality of the catalytic site was reported as favourable for efficient catalysis [27]. In MDH, the double negative charge of OAA is screened by R102 and R171, once the catalytically competent complex is formed, ensuring the neutrality within the catalytic site [32, 38]. In LDH, the single negative charge of the D199 lateral chain and that of PYR ensure the neutrality of the catalytic site. The presence of D199 (or E199) is therefore considered as a one of the specific signatures for LDH, while the presence of a neutral amino acid at the equivalent position (e.g. M199) is associated to MDH. According to these ~~those~~ studies, the nature of the amino acids at these three positions could be used to distinguish LDH and MDH. Yet, these assumptions are mostly based on the analysis of a few enzymes and do not embrace the huge diversity of the LDH / MDH3 family. For instance, the observation of M199 in MDH relied on a comparison between LDH and (dimeric) MDH1 and MD2, when MDH3 were unknown [27]. Furthermore, several recent reports suggested that the situation could be more complex. For instance, MDH3 from *I. islandicus*, which displays R102, A199, and T246 as sequence signature, is able to recognize both OAA and PYR as substrate [19]. In addition, the recognition of PYR by LDH in apicomplexa differs from the one existing in canonical LDH. In fact, in these eukaryotes the functional shift from MDH toward LDH activity is due to a six amino acids insertion in the mobile loop that covers the catalytic site upon substrate binding [39, 40]. The insertion induces a structural reorganisation that dramatically changes the location of the residue at position 102, which consequently protrudes outside the catalytic vacuole and lost its critical role of discriminating residue. A detailed evolutionary scenario by which apicomplexa LDH could have acquired the capacity to recognize PYR has been recently proposed [22].

Here, we present a large scale phylogenomic analysis of the LDH / MDH superfamily. The inferred phylogenies reveal a complex evolutionary history, heavily impacted by horizontal gene transfer (HGT) across and within the three Domains of Life. The mapping of the discriminating amino acids at positions 102, 199, and 246 discloses a large group of LDH / MDH3 sequences harbouring unexpected combinations of amino acids. This group of

sequences occupied an intermediate position between *stricto sensu* MDH3 and LDH enzymes. Functional characterizations reveal that members of this group are very diverse and harbour original enzymatic properties, combining LDH and MDH features, as exemplified by the enzyme from *Tolumonas auensis*. The present work shows that the LDH / MDH3 family is more diverse than previously expected and that the emergence of *stricto sensu* LDH occurred from this intermediate group by a three-step acquisition and fixation of critical residues in the active site.

2. Materials and methods.

2.1. Identification of the LDH / MDH superfamily members

A local protein sequence database gathering the 16,052 reference proteome sequences from UniProt (https://www.uniprot.org/proteomes/) was built. More precisely, this corresponded to 433 archaea, 8,593 bacteria, 1,142 eukaryotes, and 5,884 viruses proteomes (Supplementary Table S1A). The local database was queried with HMMER 3.1b2 [41] using the two Hidden Markov Models (HMM) profiles from the PFAM v32.0 database that target the N-terminal and the C-terminal parts of sequences belonging to the LDH / MDH superfamily: the lactate / malate dehydrogenase NAD binding domain (Ldh_1_N, PF00056) and the lactate / malate dehydrogenase alpha / beta C-terminal domain (Ldh_1_C, PF02866) [42]. This revealed 12,983 sequences containing both domains (*Evalue* threshold = 10^{-2}) (Supplementary Table S2). The length of the retrieved sequences ranged from 113 to 2,428 amino acids positions (average length = 331 amino acid positions).

2.2. Phylogenetic analysis of the lactate / malate dehydrogenase superfamily

The 12,493 sequences longer than 230 and shorter than 430 amino acid positions were aligned with MAFFT v7.453 [43] using the --auto and --reorder options. The resulting multiple alignment was used to infer a phylogenetic tree using FASTTREE v2.1.9 [44] with the Le and Gascuel (LG) evolutionary model [45], and the -gamma and -cat = 4 options. Branch supports were estimated using the Shimodaira-Hasegawa (SH) test implemented in FASTTREE.

2.3. Phylogenetic analysis of LDH / MDH3 family

To avoid taxonomic redundancy, a sampling of 266 eukaryotic, 269 archaeal, and 1,737 bacterial proteomes was performed by keeping randomly at least one representative strain per genus (Supplementary Table S1B). These 2,272 proteomes contained 1,635 LDH / MDH3 protein sequences longer than 230 and shorter than 430 amino acid positions. These sequences were aligned with MAFFT v7.453 with the L-INSI option that allows the

construction of accurate multiple alignments [43]. The resulting alignment was trimmed with BMGE v1.2 [46] with the BLOSUM30 substitution matrix and used to build a Maximum Likelihood (ML) tree. The phylogeny was inferred with the IQ-TREE program v1.6.12 [47]. The LG model with a gamma distribution (G4, 4 categories, estimated alpha parameter) was identified by ModelFinder [48] as the most suitable for the tree reconstruction. Branch supports were estimated by the ultra-fast bootstrap procedure implemented in IQ-TREE (1,000 replicates).

2.4. Tree drawing, residue mapping, and heatmap

Tree figures were drawn with iTOLv4 [49]. Heatmaps were built using ClustVis [50].

2.5. Residue numbering

The numbering of residues is defined with respect to the first structure of an LDH [37]. This common numbering scheme allows one to recognize easily important active site residues, such as R109, D168, R171 and H195, which are strictly conserved in all MDH and LDH.

2.6. Protein expression

Sixteen genes belonging to the LDH / MDH3 family have been chosen for functional investigations. Seven genes code for proteins from mesophilic strains (set 1): *Methanosarcina mazei* DSM 3647 (UniProt ID Q8PVJ7) *Planctopirus limnophila* strain ATCC 43296 (UniProt ID D5SXK9), *T. auensis* TA4 (UniProt ID C4LFJ3), *Selenomonas ruminantium* (UniProt ID Q9EVR0), *Methyloprofundus sedimenti* (UniProt ID A0A1V8M393), *Cellulosilyticum lentocellum* strain ATCC 49066 (UniProt ID F2JLM3), and *Teredinibacter turnerae* strain ATCC 39867 (UniProt ID C5BM91), while nine others genes code for enzymes from (hyper)thermophilic strains (set 2): *Aquifex aeolicus* strain VF5 (UniProt ID O67655), *Thermaerobacter marianensis* strain ATCC 700841 (UniProt ID E6SLT2), *Thermosinus carboxydivorans* Nor1 (UniProt ID A1HSK3), *Ignicoccus hospitalis* strain KIN4/I (UniProt ID A8ABY7), *Pyrobaculum aerophilum* strain ATCC 51768 (UniProt ID Q8ZVB2), *Methanopyrus kandleri* strain AV19 (UniProt ID Q8TWG5), *Nitrososphaera viennensis* EN76 (UniProt ID A0A060HG74), *Ca*. 'Bathyarchaeota archaeon' RBG_13_46_16b (UniProt ID A0A1F5CVF0), and *Pyrolobus fumarii* 1A (UniProt ID G0EHD0).

In addition, two genes coding for enzyme previously characterized, the HicDH from the mesophilic *Weissella confusa* LBAE_C39_2 (UniProt ID H1X598) and the MDH3 from the hyperthermophilic *Methanocaldococcus jannaschii* ATCC 43067 (UniProt ID Q60176), used as tetramer control, were cloned and once purified their products were used as tetrameric markers for calibration in Size exclusion chromatography and SEC-MALLS (see below).

The eighteen genes have been synthesized by the Genecust company. The sequences were subjected to codon optimization for over expression in *Escherichia coli.* In order to facilitate the purification using affinity chromatography, an extension of six histidine was fused to the C-terminus of mesophilic enzymes (set 1), while the products of other genes (set 2) were synthesized without any extension. All the enzymes were sub-cloned into the pet20a vector between the *NdeI* and *BamHI* restriction sites. The constructs were transformed into BL21(DE3) plysS cells and selected on LB-agar plate containing 100 ug ml-1 ampicilin. A single colony was cultured overnight at 37°C in 100 ml LB medium containing 100 ug ml-1 ampicilin. 25 ml of this culture were transferred into 1L of LB medium containing 100 ug ml-1 ampicilin. The cells were grown at 37°C until an OD600 of 0.6 was reached.

At this step, the overexpression protocol differs between set 1 and set 2.

For set1, the temperature was quickly lowered to 4°C and the cells were kept on ice for three hours, then IPTG was added at a final concentration of 0.2 mM to induce expression, which was continued overnight at 20°C. For set 2, IPTG was added to 0.5 mM and the cell cultivation was continued for four hours at 37°C. For both sets of enzymes, bacterial cells were harvested by centrifugation. The pellets were suspended in 50 m*M* Tris-HCl pH7, 50 mM NaCl (Buffer A) and frozen at -20°C for storage.

2.7. Standard enzymatic assays.

MDH activity was assessed by measuring the initial rates of OAA reduction (NADH or NADPH oxidation) at 340 nm in a thermostated spectrophotometer from JASCO. The standard assay mixture contained 50 mM Tris-HCl pH 7.2, 50 mM NaCl, 0.3 mM coenzyme and the enzyme in a final volume of 1 ml. The reaction was initiated by addition of OAA at a final concentration of 0.3 mM.

LDH activity was assessed in the same manner. The standard assay mixture contained 50 mM MES pH 6.2, 50 mM NaCl, 0.3 mM coenzyme and the enzyme. The reaction was initiated by addition of PYR. Two concentrations of 1 and 10 mM were tested. The MDH and LDH assays were carried out at 40°C or 70°C with enzymes considered as mesophilic or thermophilic, respectively. One unit of MDH or LDH activity corresponds to the amount of enzyme that catalyzes the oxidation of 1 micromole of NADH per min.

2.8. Protein purification

For set 1, after thawing of the cells, DNase at 5ug ml-1 was added to the suspension. The cell suspension was sonicated with a Branson sonicator at 25% intensity during three cycles of 1min. The extract was centrifuged at 18,000g for 30 min at 4°C. The supernatant was filtered on a 0,45 um (amicon), It was passed through a 5mL HisTrap Q HP column (GE Healthcare Life Science). The column was washed with 20 mL of 50 mM Tris-HCl pH7, 200

mM NaCl and by 20 mL of 20 mM imidazole pH 7, 200 mM NaCl. Then, the protein under study was eluted with 300 mM imidazole pH 7, 50 mM NaCl. The protein was concentrated and dialyzed in Buffer A with Amicon Ultra-30 concentrators. The protein was then loaded on an anion exchange UnoQ (BioRad) and eluted with a linear gradient from 0 to 1M NaCl buffered by 50 mM Tris-HCl pH7. The active fractions were pooled, concentrated and loaded on a size exclusion chromatography column (SEC) equilibrated with buffer A. A Superose 12 (GE Healthcare Life Science) or an Enrich 650 (Biorad) column were used. Fractions containing the enzymes under study were concentrated and stored at -80°C in buffer A with 20% glycerol.

For set 2, the crude extract preparation was as described with set 1. Due to the expected thermophilic properties of these enzymes, the soluble fraction was incubated at 75°C for 30 minutes and centrifuged at 18,000g for 30 minutes. The clear supernatant was loaded on a Q sepharose (2x5cm) and eluted using a linear gradient of gradient from 0 to 1M NaCl buffered by 50 mM Tris-HCl pH7. The end of the purification procedure using SEC and the storage were as with set 1. In the case of the *M. kandleri* sequence, the SEC column was equilibrated in a 0.4 M NaCl, Tris-HCl 50 mM pH7.

Each recombinant MDH3 and LDH purification yielded 10 mg of pure enzyme that was used for characterization.

2.9. Determination of native molecular masses of the purified enzymes.

Size Exclusion Chromatography was carried out with a flow rate of 0.5 $mL.min^{-1}$ on an Enrich 650 column (Biorad). Calibration of the column was performed with the gel filtration standard from Biorad. Direct comparison of the elution profiles was achieved using the Compare mode of the BioLogic FPLC operating system (Biorad).

2.10. Size Exclusion Chromatography - Multi Angle Laser Light scattering (SEC-MALLS).

SEC combined with online detection by MALLS and refractometry (RI) was used to measure the absolute molecular mass of proteins in solution. The SEC run was performed using an ENrich^{TM} SEC650 10x300 gel-filtration column (Biorad) equilibrated with a buffer composed of 50 mM Tris-HCl pH7.2 and 50 mM NaCl. Separation was performed at room temperature and 50 µl of protein sample, concentrated at ~5 mg ml^{-1}, was injected with a constant flow rate of 0.5 ml^{-1} min^{-1}. Online MALLS detection was performed with a DAWN-HELEOS II detector (Wyatt Technology Corp.) using a laser emitting at 690 nm. Protein concentration was determined by measuring the differential refractive index online using an Optilab T-rEX detector (Wyatt Technology Corp.) with a refractive index increment *dn/dc* of 0.185 ml^{-1} g^{-1}.

Weight-averaged molecular weight (Mw) determination was done with the ASTRA6 software (Wyatt Technologies) and curve was represented with GraphPad Prism.

2.11. Analytical ultra-centrifugation.

Ultra-centrifugation experiments were conducted in an XLI analytical ultracentrifuge (Beckman, Palo Alto, CA) using an ANTi-50 rotor, using double channel Epon centerpieces (Beckman, Palo Alto, CA) of 12 mm optical path length equipped with sapphire windows, with the reference channel being typically filled with the solvent of the sample. Acquisitions were done at 20°C and at 42,000 rpm (130,000g), overnight, using absorbance (280 nm) and interference detection. Data processing and analysis was done using the program SEDFIT [51], and GUSSI [52] using standard equations and protocols [53].

2.12. Kinetics parameters.

For each experiment assay, initial rates of NADH or NADPH oxidation were recorded at various concentrations of OAA and PYR. The concentration of NADH and NADPH was 0.2mM. The data were analyzed using Graph Pad Prism V6 using the Michaelis-Menten or Allosteric sigmoidal option. Because of the difficulties to determine the exact Km values gained for kinetics at very low substrate concentration, the values reported here correspond to an apparent Km.

3. Results.

3.1. The LDH / MDH superfamily has a complex evolutionary history

A survey of 16,052 reference proteomes covering the three Domains of Life and Viruses (i.e. 433 archaea, 8,593 bacteria, 1,142 eukaryotes, and 5,884 viruses) identified 12,983 LDH / MDH homologues with an average length of 331 amino acids positions in 7,575 proteomes (47.2%) (Supplementary Tables S1 and S2). More precisely, 290 homologues were detected in *Archaea*, 8,010 in *Bacteria*, 4,683 in *Eucarya*, while none were present in viruses (Supplementary Tables S1A and S2). Among them, 490 (3.78%) have unexpected length (less than 230 or more than 430 amino acid positions), whereas the 12,493 other sequences have a size compatible with LDH and MDH enzymes: 288 in *Archaea*: 7,978 in *Bacteria*, and 4,227 in *Eucarya*. The phylogenetic analysis of these sequences recovered three major clusters, corresponding to dimeric MDH1 and MDH2 enzymes (2,792 sequences, SH support = 0.991, and 2,571 sequences, SH support = 0.936, respectively), and a large clade corresponding to tetrameric MDH3, HicDH, and LDH enzymes (7,130 sequences, SH support = 0.892) (Figure 1). These three families displayed very different taxonomic distributions (Figure 2A-D). In fact, MDH1 are mainly present in *Bacteria*, MDH2 in

Eucarya, while LDH / MDH3 are broadly distributed in the three Domains of Life. As a consequence, the tree Domains of Life harbour different profiles (Figure 2E-H): LDH / MDH3 prevail in *Archaea* and *Bacteria*, MDH2 are abundant in *Eucarya*, whereas MDH1 are majority in *Bacteria*.

The phylogenetic analysis of the LDH / MDH superfamily showed major inconsistencies with the current systematics. In fact, bacterial, archaeal, and eukaryotes sequences are mixed in the tree, indicating that inter-domain HGT occurred (Figure 1). Furthermore, the taxonomic distribution of MDH1, MDH2, MDH3, and LDH is highly variable depending on the considered lineages (Figure 3). For instance, regarding the *Planctomycetes*, *Verrucomicrobia*, and *Chlamydiae* (PVC) superphylum, MDH1 dominates in *Chlamydiae* and *Verrucomicrobia*, while MDH3 is majority in *Planctomycetes*. Worth to note, while both cytosolic MDH1 and mitochondrial MDH2 were likely inherited in eukaryotes from their last common ancestor, these enzymes are not universal in present-day lineages, suggesting that secondary and independent losses occurred during the diversification of *Eucarya*. Yet, all eukaryotic lineages encode at least one of these two MDH, to the exception of most apicomplexan that have neither of them, and instead harbour a MDH3 likely acquired from a bacterial donor (Figures 3A and 4). This suggests that the native MDH1 and MDH2 enzymes were secondary replaced by MDH3 in the Apicomplexa. Furthermore, the number of LDH / MDH is highly variable even at small evolutionary scale, within species and genera (Supplementary Table S1A). As an example, *Klebsiella pneumoniae* subspecies pneumoniae and *Klebsiella oxytoca* harbour two homologues, while a single homologue is found in *Klebsiella aerogenes* and *Klebsiella pneumoniae* ISC21, and none is present in *K. pneumoniae* strains IS39, IS43, and IS46. This suggests that the evolutionary history of LDH / MDH enzymes is complex and may have been also heavily impacted by gene loss in addition to HGT.

To go further, we performed an accurate ML phylogenetic analysis of each of the three families. To limit taxonomic redundancy, we sampled the 16,052 reference proteomes by keeping one or two representative strains per genus. The 2,272 retained proteomes (266 eukaryotes, 269 archaeal, and 1,737 bacterial) contained 602 MDH1, 561 MDH2, and 1,635 LDH / MDH3 sequences longer than 230 and shorter than 430 amino acids. The resulting trees confirmed that the evolution of the LDH / MDH has been heavily impacted by HGT and revealed puzzling patterns (Supplementary Figures S2-S4). For instance, most bacterial sequences from different phyla are intermixed on the trees and do not form monophyletic groups as expected if they have had vertical inheritance (Supplementary Figures S2A, S3A, and S4A). A similar situation is observed for archaeal LDH / MDH3, the main protein family present in *Archaea*. In fact, LDH / MDH3 sequences are patchily distributed across archaeal lineages (Figure 3C), and their phylogenetic relationships are at odds with the current archaeal systematics (Supplementary Figures S4C).

3.2. Eukaryotic MDH / LDH have not been acquired from archaeal ancestors or through the mitochondrial endosymbiosis

Regarding eukaryotic sequences, one would expect a close relationship between eukaryotic cytosolic MDH1 and archaeal enzymes if the former had been inherited from the archaeal lineage at the origin of eukaryotes on the one hand, and a close relationship between mitochondrial MDH2 and alphaproteobacterial sequences in agreement with the mitochondrial endosymbiosis hypothesis on the other hand [54]. The analysis of the MDH1, MDH2, and LDH/MDH3 families provided a very different picture.

The MDH1 family gathers mainly actinobacterial, PVC, gammaproteobacterial, and betaproteobacterial sequences, whereas it is patchy distributed in a few archaea and alphaproteobacteria (Figure 3). Furthermore, these sequences do not display any specific link with eukaryote sequences (Supplementary Figure S2B). This precludes the possibility that the cytosolic MDH1 of eukaryotes have been acquired vertically from *Archaea* or through the mitochondrial endosymbiosis. In fact, MDH1 have been likely acquired by eukaryotes via HGT from a non-alphaproteobacterial bacterial donor. Because MDH1 sequences from eukaryotes are not specifically linked to any specific bacterial lineage, the identity of the bacterial donor lineage cannot be determined.

Regarding MDH2, this family encompasses very few bacterial sequences, mainly from gammaproteobacteria, and none are present in *Alphaproteobacteria* or *Archaea* (Figures 1 and 3, and Supplementary Figure S2). This suggests either a gammaproteobacterial origin of eukaryotic mitochondrial MDH2 or an HGT event from eukaryotes to gammaproteobacteria followed by HGT among gammaproteobacterial lineages. Altogether, an alphaproteobacterial or an archaeal origin of eukaryotic MDH1 and MDH2 is excluded. Puzzlingly, while most alphaproteobacterial proteomes contain LDH / MDH3 sequences, they are unrelated to eukaryotic sequences (Figure 3 and Supplementary Figure S4). This means that if eukaryotes have acquired an alphaproteobacterial LDH / MDH3 coding gene through the mitochondrial endosymbiosis, it has been lost, possibly after the acquisition of a MDH2 from bacterial, as proposed early on by Madern (2002).

Eukaryotic proteomes from some alveolata, fungi, metazoa, and viridiplantae contain LDH / MDH3 sequences (Figure 3). These sequences are intermixed with prokaryotic sequences reflecting again secondary and independent acquisitions by HGT from different donors (Figure 1 and Supplementary Figure S4). In the case of apicomplexa, a subsequent neofunctionalization event allowed their MDH3 to acquire the capacity to converts PYR to lactate [22].

3.3. Mapping of residues involved in substrate recognition sheds a new light on the LDH / MDH3 family

The LDH / MDH3 family encompasses LDH, MDH, and the enigmatic HicDH enzymes. The unrooted phylogeny of this large family does not clearly distinguish subfamilies that would correspond to these three enzymes (Supplementary Figure S4). Previous experimental works have shown that substrate discrimination depends strongly on the conformation of the substrate-binding site and thus on the nature of the residues present, with canonical MDH3 harbouring R102, A246 or S246, while canonical LDH Q102 and T246 at the homologous sites. In addition, canonical LDH have an acidic residue (aspartate or glutamate) at position 199. We mapped these residues on the LDH / MDH3 phylogeny, as well as the phylogenetic position of characterized enzymes (Figure 4A). As expected, the nature of these three residues involved in lactate or malate production and experimental data were consistent (see filled / empty blue triangles as well as filled / empty grey triangles on Figure 4A). Consistently, two large clades corresponding to LDH and MDH3 can be delineated (clades with blue and pink branches on Figure 4A, respectively), and will be hereafter referred as to LDH and MDH3 *stricto sensu*. These two clades are homogenous regarding the nature of the residue at position 102, to the exception of apicomplexan LDH sequences that are nested within MDH3 *stricto sensu* sequences. This is not surprising because these eukaryotes LDH result ~~of~~ from a recent neofunctionalization event of a MDH3 enzyme involving structural changes of the catalytic site. As a consequence, the R102 residue has lost its role in substrate discrimination (see above). Another exception concerns a small group of sequences nested within *stricto sensu* LDH that display residues typical of MDH3 enzymes at position 102 and 246. LDH *stricto sensu* sequences are mainly present in bacteria, some eukaryotes (i.e. in some metazoa, viridiplantae, fungi, and in a few protists), and in a few archaea, while MDH3 sequences are mainly present in bacteria (Figure 4A).

Surprisingly, a large group of sequences branch in-between *stricto sensu* LDH and MDH3 sequences (Figure 4). Sequences from this intermediate group harbour different combinations of amino acids at positions 102, 199, and 246 (Figures 4A and 4B). In fact, most of these sequences harbour only one residue involved in PYR recognition (T246), associated in some cases to residues specifically associated to OAA recognition (i.e. R102) or to PYR recognition (i.e. D199 or E199). They encompass most archaeal sequences and a mix of bacterial sequences from different phyla (Figure 4B). Notice that LDH enzymes from *Thermotogales* are nested within the intermediate group and not within the *stricto sensu* LDH, although they display their three amino acids signature (Figure 4B). According to the literature, this intermediate group contain enzymes using OAA and PYR as substrate, as well as HicDH (empty and filled grey triangles on Figure 4B, respectively). Yet, functional data are scarce and do not encompass the whole diversity of the group, especially regarding the

nature of the amino acids observed at the three important positions for substrate discrimination.

3.4. Functional characterization reveals new unexpected enzymatic properties.

To go further, we characterized enzymes occupying key positions in the LDH / MDH3 family and/or harbouring various and original amino acid combinations at critical positions 102, 199, and 246 with the aim to increase the description of the LDH / MDH3 family, and especially the intermediate group (Table 1). More precisely we selected three enzymes belonging to group of MDH3 *stricto sensu*: *A. aeolicus* strain VF5, *T. marianensis* strain ATCC 700841, and *M. mazei* DSM 3647, to enrich the functional information for this very large cluster (Figure 4A). We selected also *P. limnophila* ATCC 43296 as representative of the enigmatic small subgroup of sequences nested within LDH *sensu stricto* that harbor amino acids associated to MDH3 (i.e. R102, M199, and A246) instead of the three residues associated to PYR recognition (i.e. Q102, T246 and D/E199) (Figure 4A). Regarding the intermediate group, functional data are available in the literature for a few members of subgroups C, E, G, H, I, J, and one enzyme located in-between subgroups H and J (empty and filled grey triangles on Figure 4B and Supplementary Table S3). In this study, we investigated the properties of twelve additional enzymes from the intermediate group: *N. viennensis* and *Ca*. 'Bathyarchaeota archaeon' RBG_13_46_16b (subgroup A), *P. aerophilum* strain (subgroup B), *T. carboxydivorans* Nor1 (a lonely sequence located in-between subgroups E and F), *T. auensis* (subgroup F), *M. kandleri* (subgroup I), *I. hospitalis* (subgroup J), *P. fumarii* (subgroup J), *S. ruminantium*, *C. lentocellum*, *T. turnerae*, and *M. sedimenti* (subgroup L) ~~(Table 1)~~.

To determine whether the products of the sixteen selected genes, corresponding to three MDH3 *stricto sensu*, one LDH *stricto sensu*, and twelve sequences from the intermediate group, could be assigned as MDH or LDH, the overexpressed soluble proteins were purified, their oligomeric state was determined, and their capacity to use OAA or PYR was tested. Among the selected targets, six from the intermediate group (i.e. the two enzymes from subgroup A and some of subgroups J and L) did not fold properly after overexpression in *Escherichia coli*.

3.4.1. Determination of the oligomeric state

Elution profiles of the properly folded enzymes showed a major peak on SEC column suggesting it contains a single oligomeric species. The *M. jannaschii* MDH3 (subgroup I) and *W. confusa* HicDH (subgroup P), for which the crystal structures indicate that they are tetramer were used as control experiments [55, 56]. Both enzymes display an elution volume around 13.5 mL (see I and J panels on Supplementary Figure S5). To the exception of the

T. auensis enzyme, which has a higher elution volume of 14,5 mL suggesting it behaves as a dimer, the other enzymes display elution volume similar to the control experiments indicating that they are tetramers. Because the determination of molecular weight of a protein by SEC is sensitive to several artefacts [57], eight measurements were completed by SEC MALLS analysis (Supplementary Figure S6). The eight enzymes analysed (including the *M. jannaschii* MDH3 as control) display molecular weights in agreement with the tetrameric state. The specific case of *T. auensis* enzyme, which was disclosed as dimer is presented below. Altogether, these data confirm that the tetrameric association is likely dominant within the MDH3 / LDH clade.

3.4.2. Determination of the functional activity

Then, proteins under study were assessed for their capacity to recognize OAA and PYR with NADH or NADPH as coenzyme. To the exception of *S. ruminantium*, which uses only PYR and should be considered as an LDH, the other enzymes strictly use OAA MDH. Saturation curves are presented and maximal specific activity have been determined (Table 1 and Supplementary Figure S7). The enzymes shown to used OAA harbor profiles expected for Michaelian enzymes with either a hyperbolic profile or a profile showing an inhibition by increasing concentration of substrate. Activity values are in the typical data ranges reported for MDH [58] to the exception of *P. limnophila* and *T. auensis*, which have maximal specific activity below 100 U. mg^{-1}.

As expected, activity measurements confirm that enzymes from *A. aeolicus*, *T. marianensis*, and *M. mazei*, belonging to the clade of *stricto sensu* MDH3, are functional tetrameric MDH, which use OAA as substrate and NADH as coenzyme, an observation in agreement with the presence of R102, M199, and A246, and with previous measurements on bacterial sequences from the MDH3 clade [59-61]. A malate activity, albeit with a low specific activity, is also observed for the *P. limnophila* enzyme. The corresponding sequence is nested within *stricto sensu* LDH but harbor, R102, M199, and A246 like most MDH3 - and not the three LDH residues associated to PYR recognition. This strongly suggests that a shift from lactate toward malate production occurred, likely as a consequence of the replacement of the three residues favoring PYR recognition by amino acid favoring OAA recognition. To our knowledge, this is the first report of a functional shift from LDH toward MDH activity.

Within the intermediate group, subgroups B and I harbor R102, M199, and A246 (or S246), found in MDH3 *stricto sensu* enzymes. Consistently, *P. aerophilum* and *Aeropyrum pernix* enzymes (subgroup B), and and *M. kandleri* enzymes (subgroup I) use OAA as substrate (Table 1 and Supplementary Table S3). However, while the two enzymes of subgroup B use only NADH as coenzymes, the enzymes of *M. jannaschii* (subgroup I) and *Methanothermobacter thermoautotrophicus* (subgroup H) use both NADH and NADPH with a

preference for the latter [62, 63]. Activity measurements using the *M. kandleri* enzyme (subgroup I), confirms it is a NADPH-dependent MDH. The strict preference for NADH in dehydrogenase relies on the presence of an aspartate at the position 52 (Supplementary Figure S8) in the coenzyme binding site that prevents, owing to electrostatic repulsion, the binding of the additional phosphate in NADPH [64]. In *Methanothermobacter thermoautotrophicus*, *M. jannaschii*, and *M. kandleri* sequences a glycine (neutral residue) is present at position 52, allowing accommodating the NADPH. Most sequences LDH / MDH3 family harbour D52. The presence of alternative residues (mainly glycine or serine) at position 52 is restricted to sequences of subgroups H, I, and K, a few members of subgroup L (not shown). This suggests that the use of NADPH is rather rare and that this feature emerged recently and independently during the diversification of the LDH / MDH3 family.

Interestingly, sequences from subgroups C, E, H, J, and the two sequences located in-between E and F subgroups harbour R102 typical of MDH3 *sensu stricto* and T246 specific of LDH enzymes, while various residues are observed at position 199 (e.g. A199, Q199, or M199). Accordingly, we wondered the impact of this mix combination of MDH and LDH signatures on the activity of these enzymes. Previous reports indicate that *A. fulgidus* (subgroup C), *Haloarcula marismortui* (subgroup E), as well as *Metallosphaera sedula* and *I. islandicus* (both from subgroup J) have an NADH-dependent MDH activity with high activity for OAA. Our data indicate that this is also the case for *T. carboxydivorans*, an enzyme that branch in-between E and F subgroups and that shows an MDH activity with a low affinity for OAA (i.e. K_m values higher than 0.5 mM) (Table 1). Accordingly, it would be tempting to conclude that the presence of R102 has a stronger influence than T246 on substrate recognition, and that subgroup A and O enzymes could have MDH activity. However, in a recent study, the NADH-dependent MDH3 from *I. islandicus* was shown to use OAA (with high affinity) but also PYR in the absence of OAA to produce lactate yet with very low affinity and efficiency [19]. The structure of this enzyme has revealed a slight deformation of the catalytic site compared to other enzymes harbouring the same combination of amino acids at positions 102, 199, and 246, and changes of the relative orientation between subunits that make the tetrameric scaffold. It has been proposed that these features are responsible for the dual activity [19]. The situation is likely more complex, ~~as~~ since we show here that the enzyme from *I. hospitalis*, a close relative of *I. islandicus*, strictly recognizes OAA (Supplementary Figure S7). Both enzymes share the same three amino acids signature (R102, A199, T246), but diverge by 55 amino acid replacements. These changes may impact the local topology and dynamics of their catalytic site, making them more or less efficient in substrate differentiation. This illustrates that functional differences may exist even at small evolutionary scale. This indicates that even if amino signatures are good predictors of

substrate recognition and enzymatic activity, they are not sufficient, especially in the case of enzymes with dual activities.

Puzzlingly, most of the sequences of the intermediate group harbour neither arginine nor glutamine at amino acid position 102, whereas all of them harbour either a threonine at position 246 as LDH or a serine at the equivalent position as MDH3. This is surprising given the important role of the position 102 in substrate differentiation, but it opens the possibility to investigate the contribution of amino acid at position 246. More precisely, most enzymes harbour a threonine at position 246 (sequences belonging in-between subgroups H and I, and in subgroups L, N, and P), while the presence of S246 is restricted to sequences from the subgroup F. Functional information on those sequences are rare. Regarding sequences harboring T246, available data rely on the characterization of the HicDH of *W. confusa* [65] and *Mycoplasma agalactiae* PG2 [66]. Both enzymes display a PYR-dependent LDH activity, even if the HicDH recognizes preferentially branched oxoacids and to a lesser extent PYR. The comparison between structures of *W. confusa* HicDH and some LDH showed that it is the consequence of hydrophobic changes in the substrate binding pocket, which direct substrate specificity towards large substrate [56]. Here we have performed the characterization of a representative of the large subgroup L, the enzyme of *S. ruminantium*. Our data indicates that this enzyme is an LDH with a low affinity for PYR. This is consistent of the indirect assignation of the *S. ruminantium* enzyme as a LDH because of its capacity to complement the anaerobic growth deficiency of an *E. coli* mutant [67]. We noticed that in this protein, the three amino acids signature is I102, A199 and T246. In order to establish firmly its function, the gene product was overexpressed and purified. The protein is a tetramer as analyzed with SEC MALLS (Table 1 and Supplementary Figure S6). It uses only NADH as coenzyme and recognizes PYR with a sigmoid profile (Table 1 and Supplementary Figure S7). The affinity for PYR is 2 mM and FBP does not exert any activation. The Hill' coefficient was 2.5. OAA was not recognized. The characterization demonstrates that the enzyme of *S. ruminantium* is therefore an LDH of low affinity for PYR that displays homotropic activation. The characterization of the *S. ruminantium*, *Mycoplasma agalactiae*, and *W. confusa* enzymes suggests that the presence of a threonine at amino acid position 246 associated to the absence of R102, could be sufficient to abolish the recognition of OAA and to induce an affinity for PYR. However, additional data is needed to test this hypothesis.

3.5. The puzzling enzyme from *Tolumonas auensis*

The case of *T. auensis* within subgroup F is of special interest because it harbours a P at position 102, while other sequences of subgroup F have a glycine, an alanine or a serine. Amino acid at position 102 is part of the mobile loop that covers the catalytic site upon substrate binding. Because of its intrinsic structure, a proline residue decreases the local

flexibility of the protein backbone [68]. Consequently, it is likely that P102 could strongly influence the substrate differentiation capacity of the *T. auensis* enzyme, even if amino acid at position M199 and S246 correspond to those generally encountered in *sensu stricto* MDH3. The inspection of the *T. auensis* enzyme primary sequence showed also a noticeable exception with respect to the putative coenzyme utilization. While, all LDH and most MDH3 harbor D52 in agreement with their capacity to use NADH [64] (see above), *T. auensis* and other members of subgroup F display an asparagine at the equivalent position, suggesting these enzymes preferentially uses NADPH. Because of this atypical combination of amino acids, the enzyme of *T. auensis* was therefore purified and characterized.

Surprisingly, the elution profile using SEC at the end of the purification revealed that the enzyme elutes at 14.5 mL (Supplementary Figure S5). Such a value suggests that the enzyme does not behave as a tetramer (see above). The oligomeric state of the enzyme was further analysed using SEC-MALLS and by analytical ultra-centrifugation. Its theoretical molecular weight is 138 kDa for a tetrameric association. The protein elutes as a single peak on SEC with an elution volume of 13.8 ml. The experimental weight-averaged molecular mass was 56.4 ± 5 kDa (Figure 5A). Such a value is consistent with a dimeric species instead of a tetramer. The *T. auensis* enzyme oligomeric state was also analyzed using ultra-centrifugation. The sedimentation coefficient $S_{20,w}$ profile shows a major peak of 4.67 +/- 0.2 S with a frictional coefficient ratio of 1.29 that confirms it is a globular dimer (Figure 5B). Previous studies using ultra-centrifugation showed tetrameric MDH3 have $S_{20,w}$ values in the range 7.0-7.2 S [19, 69].

The experimental data show that the enzyme is able to reduce both OAA and PYR with NADPH (0.3 mM), but not with NADH. This dual capacity of substrate recognition strongly suggests a phenomenon of promiscuous enzymatic activity that could be due to the absence of canonical discriminating residue Q or R at position 102. The W. conf HicDH with no canonical (OAA/PYR) substrate discriminating residue at position 102 was shown to be able to use 2-Oxoisocaproate 2-oxocaproate, 2-phenylpyruvate in addition to PYR (Feil, et al. 1994). None of these compounds were recognized by the T. aue enzyme.

In the presence of OAA, the hyperbolic profile for activity of the enzyme is consistent with an MDH profile. It has a maximal activity of 19 $U.mg^{-1}$ and a K_m value for OAA of 8.5 mM (Figure 5C). Such a K_m value demonstrates a very low affinity for OAA, in contrast to most of *stricto sensu* MDH3 for which K_m for OAA is below 0.3 mM [19, 58]. The capacity of OAA recognition by the enzyme of *T. auensis* is consistent with the presence of a serine at position 246, as in MDH3 enzymes. Unexpectedly, this enzyme catalyzes also PYR oxidation using NADPH with a sigmoid profile as in the case of homotropic activation of allosteric NADH-dependent LDH [10]. The enzyme has a maximal specific activity of 94 u.mg-1, a Hill' coefficient of 1.9 and a Khalf (Km) value for PYR of 45 mM indicating a cooperative

substrate binding and a low affinity for this substrate (Figure 5D). It is assumed that the concentration of free OAA within cells of living organisms is very low, because it is continuously recycled in the TCA cycle [70]. Therefore, the functionality of the *T. auensis* enzyme as MDH is crippled by its high K_m value for OAA. In the proteome of *T. auensis*, another protein (C4LAG8 UniProt) is assigned by sequence homology to a MDH1, suggesting it acts as the "true" MDH.

With *stricto sensu* allosteric LDH, the maximal catalytically efficiency is achieved in the presence of the allosteric effector fructose 1, 6 bis-phosphate (FBP), which induces a strong favorable shift of affinity for PYR toward sub millimolar value [10]. The effect of FBP was assessed on the *T. auensis* enzyme. It did not induce any significant activation effect. Recall that in LDH, FBP binding occurs at interfaces between the dimer of dimers, which makes the final tetrameric assembly [30]. Because the *T. auensis* protein is a dimer, the condition to create an FBP-binding site is not achieved. As a conclusion of this functional investigation, *T. auensis* enzyme, displays a new unexpected behavior. It corresponds to the first description of a dimeric NADPH-dependent LDH of low efficiency that solely displays homotropic activation.

4. Discussion

Gene duplication is considered as one of the main evolutionary forces that favors the diversification of protein function [71]. A duplication event can lead to (i) the amplification of the preexisting function due to multiple copies, (ii) the specialization through the subfunctionalization of one of the two resulting paralogues, or (iii) the emergence of a novel function owing to the accumulation of key mutations via the neofunctionalization of one of the two paralogues [72]. In the super family of LDH / MDH, it was suggested that the emergence of canonical LDH resulted from the duplication of an ancestral tetrameric MDH. After the duplication, one of the paralogues kept the ancestral function and is at the origin of the MDH3 subfamily, while the second paralogue acquired the capacity to transform PYR into lactate [17].

Our in-depth investigation of the huge LDH / MDH superfamily shows that the family of LDH / MDH3 could be split into three main groups accordingly to the combination of the three amino acids involved in substrate binding and differentiation. They correspond to (i) the *stricto sensu* tetrameric MDH3 that display the combination R102, A/S246, and M199 and recognize OAA with a high affinity, (ii) an intermediate group gathering very diverse enzymes with respect to the nature of amino acids found at positions 102, 199, and 246, oligomeric states, coenzyme use, and substrate specificities and affinities, and (iii) the *stricto sensu* tetrameric LDH that mostly harbor Q102, D/E199, and T246, and that use PYR as substrate (Supplementary Table S3).

Our analysis indicates also that the evolutionary history of the LDH / MDH3 family was heavily impacted by HGT, including HGT across the three Domains of Life. Furthermore, there is no or very few taxonomic redundancies between LDH and MDH3 (Figure 4 and Supplementary Figure S4), as expected if these two subfamilies derived from a duplication event. These results challenge previous hypotheses to explain the emergence of canonical LDH and MDH3 from a duplication event [17]. A more likely scenario would be that during the diversification of MDH3, a subgroup of sequences, which is at the origin of the intermediate group, has progressively acquired the capacity to use PYR instead of OAA. A series of substitution events affecting important residues for the enzymatic activity, relaxed the strong affinity for OAA, allowing accommodating for other substrates and led to the creation of reservoir of enzymes of various oligomeric states, with different affinities and substrate differentiation capacities (Figure 6). In particular, the replacement of the alanine or the serine by a threonine at position 246, would have been a permissive event for the future evolution toward LDH. Indeed, T246 is considered as unfavorable for OAA binding [73, 74]. The conservation of R102 in archaeal proteins belonging to the intermediate group, could explain why these enzymes are always functional MDH even if they display for most of them T246. This observation confirms that R102 is the most efficient amino acid to define MDH functionality.

The role of subfunctionalization that is related to functional promiscuity cannot be ignored as playing a role in the evolution of LDH and MDH. Indeed, a previous work showed that the archaeal *I. islandicus* MDH belonging in the intermediate group has a promiscuous LDH low activity [19]. Noticed this sequence harbors threonine at position 246. The present work revealed that another enzyme from the intermediate group, C4LFJ3 from *T. auensis* (with a P102, M199, and S246 signature) could recognize both OAA and PYR, the substrates typical of MDH and LDH, with low affinity. The MDH from *T. carboxydivorans* (with a R102, M199 and T246 signature) has a low affinity for OAA, suggesting that the decrease of affinity for the main substrate of MDH was very likely one of the steps that contributed to favor the emergence of LDH. Eventually, such a phenomenon could have been amplified so that the MDH function is fully abolished. This likely happened in the subgroups of sequences that do not display an R at position 102. The characterization of the enzyme from *S. ruminantium* demonstrates it is an LDH with low PYR affinity and which no longer recognize OAA. Noticed that the subgroup G, that encompasses sequences harboring the three residues found in *sensu stricto* LDH and the experimentally characterized LDH enzyme from *Thermotoga maritima* [75], corresponds likely to LDH enzymes.

Previous studies focused the LDH / MDH superfamily indicated that LDH functionality evolved independently four times from MDH enzymes [17, 21, 22, 25]. Through the characterization of the *P. limnophila* enzyme, we disclose the first case of conversion of LDH

toward MDH. However, it occurred very rarely during the functional diversification of the LDH / MDH superfamily. By revealing new cases of functional changes from MDH toward LDH, the present work demonstrates that this phenomenon is not as rare as previously thought. These functional changes are consistent with an enzyme evolution hypothesis, which proposes that functional promiscuity and conformational diversity are strong drivers of protein evolution [76]. Accordingly, the emergence of *stricto sensu* LDH could have resulted from the neofunctionalization of an NADH-dependent enzyme, with a T246 signature, from the intermediate group with a low (or abolished) affinity for OAA and/or a low affinity for PYR. The fixation of an acidic amino acid (D or E) at position 199 promoting charge neutrality within the catalytic site and the acquisition of Q102, for which the neutral chain interacts with the neutral PYR methyl group, were the last steps to favor an efficient PYR recognition as observed in *stricto sensu* LDH. Altogether, our results confirmed that the action of mutations relies strongly on epistasis, i.e. the amplitude of the effect depends on the sequence of the rest of the protein acids [77]. This may explain why attempts to transform tetrameric MDH3 into LDH on the basis of unique R102 to Q mutation have encountered a limited success [28]. With respect to the role of the three positions analyzed in the present work, an efficient transformation would have been achieved likely, if the M199, ensuring the charge neutrality within the catalytic site, was replaced by an acidic amino acid at position 199. Finally, until the present work, the allosteric behavior was considered as constitutive of the tetrameric state in LDH, while a unique case of hidden allosteric capacity was reported for a MDH3 enzyme [19]. The characterization of the enzyme from *T. auensis* demonstrates that, in the clade MDH3 / LDH, the minimal oligomeric state which is able to support homotropic activation is a dimer.

5. Conclusion

Our phylogenetic and experimental investigations disclose an unexpected diversity of LDH / MDH3 family and shed a new light on the evolution of this important family of enzymes. In particular, we were able to characterize representative enzymes of most of the subgroups that branch in-between *stricto sensu* LDH and MDH3, yet this is far from covering the whole diversity of these atypical enzymes. Biochemical, structural and dynamical investigations of members of the intermediate group are thus of primary importance to gain insights into the evolution of allostery and substrate recognition. Our data allow us to propose an evolutionary scenario for the emergence of LDH from MDH enzymes involving punctual and permissive substitutions at key positions slightly modified and relaxed the properties of MDH enzymes. In one of these intermediate lineages, the acquisition of a few critical residues, including a glutamine at position 102, hampered the recognition of PYR, a signature of *stricto sensu* LDH.

765

766 ## Acknowledgements

767 We thank Drs Eric Girard, Fabio Sterpone, Jacques Coves, Caroline Barette, Caroline Mas,
768 and Laura Eme for stimulating discussions and critical reading of the manuscript. This work
769 used the platforms of the Grenoble Instruct center (ISBG, UMS 3518 CNRS-CEA-UJF-
770 EMBL) within the Grenoble Partnership for Structural Biology (PSB). This work also used the
771 computing facilities of the CC LBBE/PRABI.

772

773 ## Funding

774 This work has been supported by the Agence Nationale de la Recherche (ANR-16-CE11-
775 0011-02).

776 **Table 1. Summary of the experimental characterization of new members of the LDH / MDH3 family.**

Strain (Taxonomy) Accession number – key residues	Phylogenetic position	Key residues	Expected function / Real function	Coenzyme	OAA		PYR	
					Maximal specific activity (Vmax, U mg^{-1})	K_m (mM)	Maximal specific activity (Vmax, U mg^{-1})	K_m (mM)
Methanosarcina mazei (*Archaea*, *Methanosarcinales*) Q8PVJ7	MDH3 *stricto sensu*	R102, M199, A246	MDH / MDH	NADH	301	0.26	-	-
				NADPH	-	-	-	-
Thermaerobacter marianensis (Bacteria, *Firmicutes*) E6SLT2	MDH3 *stricto sensu*	R102, M199, A246	MDH / MDH	NADH	402	0.11	-	-
				NADPH	-	-	-	-
Aquifex aeolicus (*Bacteria*, *Aquificales*) O67655	MDH3 *stricto sensu*	R102, M199, A246	MDH / MDH	NADH	510	-	-	-
				NADPH	-	-	-	-
Planctopirus limnophila (Bacteria, Planctomycetes) D5SXK9	LDH *stricto sensu*	R102, M199, A246	MDH / MDH	NADH	76	0.05	-	-
				NADPH	-	-	-	-
Pyrobaculum aerophilum (*Archaea*, *Thermoproteales*) Q8ZVB2	IG – subgroup B	R102, M199, T246	MDH / MDH	NADH	254	0.10	-	-
				NADPH	-	-	-	-
Thermosinus carboxydivorans (*Bacteria*, *Firmicutes*) A1HSK3	IG – in-between E and F	R102, M199, T246	MDH / MDH	NADH	368	2.50	-	-
				NADPH	-	-	-	-
Tolumonas auensis (*Bacteria*, *Gammaproteobacteria*) C4LFJ3	IG – subgroup F	P102, M199, S246	? / LDH	NADH	-	-	-	-
				NADPH	19	8.50	94	45
Methanopyrus kandleri (*Archaea*, *Methanopyrales*) Q8TWG5	IG – subgroup I	R102, M199, S246	MDH / MDH	NADH	nd	-	-	-
				NADPH	123	0.10	-	-
Ignicoccus hospitalis (*Archaea*, *Desulfurococcales*) A8ABY7	IG – subgroup J	R102, A199, T246	MDH / MDH	NADH	253	0.18	-	-
				NADPH	-	-	-	-
Selenomonas ruminantium (*Bacteria*, *Firmicutes*) Q9EVR0	IG – subgroup L	I102, A199, T246	? / LDH	NADH	-	-	130	2.0
				NADPH	-	-	-	-

777 IG = intermediate group, nd = not determined, "-" = no significant activity detected.

778

Figure legends

Figure 1. Phylogeny of LDH / MDH superfamily.

The tree encompasses 12,493 sequences longer than 230 and shorter than 430 amino acid positions. The three main families are represented with different colours: MDH1 in brown (aLRT support = 0.936), dimeric MDH2 in purple (aLRT support = 0.991), and MDH3 and LDH (aLRT support = 0.892). Sequences from *Archaea* are represented in red, *Bacteria* in green, and *Eucarya* in orange.

Figure 2. LDH / MDH superfamily distribution in the three Domains of Life.

Taxonomic distribution of LDH / MDH superfamily across the three Domains of Life: **(A)** MDH1, **(B)** MDH2, **(C)** MDH3 / LDH / HicDH, and **(D)** all sequences. Distribution of MDH1, MDH2, MDH3 / LDH / HicDH in *Archaea* **(E)**, *Bacteria* **(F)**, *Eucarya* **(G)**, and in the three Domains of Life **(H)**.

Figure 3. Taxonomic distribution of MDH1, MDH2, LDH / MDH3 family sequences.

The colour scale indicates the proportion of proteomes containing at least one sequence of the family (white = not present, dark orange = present in all members).

Figure 4. Unrooted maximum likelihood phylogeny of the LDH / MDH3 family.

(A) Full tree showing the three main groups of LDH / MDH3 enzymes: the LDH *stricto sensu* (blue branches) that harbour the three amino acids allowing the recognition and binding of PYR (Q102, D199/E199, and T246), the MDH3 *stricto sensu* (pink branches) that harbour the two amino acids allowing the recognition and binding of OAA (R102, and SA46/S246), and the intermediate group (black branches) that harbour various combination of these amino acids.

(B) Zoom on the intermediate group. LDH and MDH3 *stricto sensu* have been collapsed.

The tree was inferred with the 1,635 sequences present in 2,272 representative proteomes.

In both trees, sequences from *Archaea* are represented in red, *Bacteria* in green, and *Eucarya* in orange. The scale bar represents the average number of substitutions per site. Circles at branch correspond to ultrafast bootstrap values. For clarity, values lower than 90% were omitted. Critical residues involved in substrate recognition and functional characterized

enzymes are mapped with dark blue triangles. The most internal circle indicates a Q (filled triangles) or a R (empty triangles) at position 102, corresponding to lactate or malate recognition, respectively. The second circle highlights a T (filled triangles) or a S/A (empty triangles) at position 246, corresponding to lactate or malate recognition, respectively. The filled triangles on third circle design an acidic residue (D or E) at position 199 that ensure charge neutrality within the catalytic site. Light grey triangles on the fourth circle design the position of experimentally characterized LDH (filled triangles) and MDH3 (empty triangles) from previous studies (Supplementary Table S3). Black triangles on the fifth circle indicate the position of experimentally characterized LDH (filled triangles) and MDH3 (empty triangles) in this study.

Figure 5. Properties of *Tolumonas auensis* enzyme.

(A) Oligomeric state determination of the *T. auensis* enzyme using SEC-MALLS analysis. The chromatogram shows the elution profile monitored by excess refractive index (left ordinate axis) and the molecular weight as dashed line (right ordinate axis) derived from MALLS and refractometry measurements. The estimated average molecular weight is indicated on the graph. **(B)** Sedimentation profile monitored by absorbance at 280 nm. **(C)** and **(D)** Enzymatic activity profiles of *T. auensis* enzyme using Oxaloacetate or Pyruvate respectively. Measurements were done in the presence of the indicated concentrations of substrates with NADPH as coenzyme.

Figure 6. Scheme of the functional evolution within the MDH/LDH superfamily.

The different groups of enzymes defined on the basis of three keys residues are indicated. The pink arrow shows the variation of oxaloacetate (OAA) affinity between the various MDHs groups: from high (solid line) to low (dashed line) values. The blue arrow illustrates the selection of LDH functionality due to pyruvate usage. The variation of the three important residues involved in substrate recognition are indicated. Only two of the various combination that can be observed within the intermediate group are shown.

Author contributions.

- conception of the work: C.B-A & D.M
- collection of data: C.B-A & D.M
- analysis of data: C.B-A & D.M
- writing of manuscript: C.B-A & D.M

Author Agreement.

All authors have seen and approved the final version of the manuscript being submitted.

References

[1] B.J. Baker, V. De Anda, K.W. Seitz, N. Dombrowski, A.E. Santoro, K.G. Lloyd, Diversity, ecology and evolution of Archaea, Nat Microbiol, 5 (2020) 887-900.
[2] J.L. Macalady, T.L. Hamilton, C.L. Grettenberger, D.S. Jones, L.E. Tsao, W.D. Burgos, Energy, ecology and the distribution of microbial life, Philosophical transactions of the Royal Society of London. Series B, Biological sciences, 368 (2013) 20120383.
[3] A. Kreimer, E. Borenstein, U. Gophna, E. Ruppin, The evolution of modularity in bacterial metabolic networks, Proceedings of the National Academy of Sciences of the United States of America, 105 (2008) 6976-6981.
[4] K.O. Alfarouk, D. Verduzco, C. Rauch, A.K. Muddathir, H.H. Adil, G.O. Elhassan, M.E. Ibrahim, J. David Polo Orozco, R.A. Cardone, S.J. Reshkin, S. Harguindey, Glycolysis, tumor metabolism, cancer growth and dissemination. A new pH-based etiopathogenic perspective and therapeutic approach to an old cancer question, Oncoscience, 1 (2014) 777-802.
[5] U.E. Martinez-Outschoorn, M. Peiris-Pages, R.G. Pestell, F. Sotgia, M.P. Lisanti, Cancer metabolism: a therapeutic perspective, Nat Rev Clin Oncol, 14 (2017) 11-31.
[6] H. Pelicano, D.S. Martin, R.H. Xu, P. Huang, Glycolysis inhibition for anticancer treatment, Oncogene, 25 (2006) 4633-4646.
[7] S.L. Zhang, Y. He, K.Y. Tam, Targeting cancer metabolism to develop human lactate dehydrogenase (hLDH)5 inhibitors, Drug Discov Today, 23 (2018) 1407-1415.
[8] M. Adeva-Andany, M. Lopez-Ojen, R. Funcasta-Calderon, E. Ameneiros-Rodriguez, C. Donapetry-Garcia, M. Vila-Altesor, J. Rodriguez-Seijas, Comprehensive review on lactate metabolism in human health, Mitochondrion, 17 (2014) 76-100.
[9] E.I. Garvie, Bacterial lactate dehydrogenases, Microbiological reviews, 44 (1980) 106-139.
[10] H. Taguchi, The Simple and Unique Allosteric Machinery of Thermus caldophilus Lactate Dehydrogenase : Structure-Function Relationship in Bacterial Allosteric LDHs, Advances in experimental medicine and biology, 925 (2017) 117-145.
[11] L.J. Banaszak, R.A. Bradshaw, Malate Dehydrogenases, in: P.D. Boyer (Ed.) The Enzymes, Academic Press, New-York, 1975, pp. 369-396.
[12] Y.M. Go, D.P. Jones, Redox compartmentalization in eukaryotic cells, Biochim Biophys Acta, 1780 (2008) 1273-1290.
[13] P. Minarik, N. Tomaskova, M. Kollarova, M. Antalik, Malate dehydrogenases--structure and function, Gen Physiol Biophys, 21 (2002) 257-265.
[14] J. Selinski, R. Scheibe, Malate valves: old shuttles with new perspectives, Plant Biol (Stuttg), 21 Suppl 1 (2019) 21-30.
[15] C. Gietl, Partitioning of malate dehydrogenase isoenzymes into glyoxysomes, mitochondria, and chloroplasts, Plant Physiol, 100 (1992) 557-559.
[16] J.J. Birktoft, R.T. Fernley, R.A. Bradshaw, L.J. Banaszak, Amino acid sequence homology among the 2-hydroxy acid dehydrogenases: mitochondrial and cytoplasmic malate dehydrogenases form a homologous system with lactate dehydrogenase, Proceedings of the National Academy of Sciences of the United States of America, 79 (1982) 6166-6170.

[17] D. Madern, Molecular evolution within the L-malate and L-lactate dehydrogenase super-family, Journal of molecular evolution, 54 (2002) 825-840.
[18] C.R. Goward, D.J. Nicholls, Malate dehydrogenase: a model for structure, evolution, and catalysis, Protein Sci, 3 (1994) 1883-1888.
[19] J. Roche, E. Girard, C. Mas, D. Madern, The archaeal LDH-like malate dehydrogenase from Ignicoccus islandicus displays dual substrate recognition, hidden allostery and a non-canonical tetrameric oligomeric organization, J Struct Biol, 208 (2019) 7-17.
[20] A. Irimia, F.M. Vellieux, D. Madern, G. Zaccai, A. Karshikoff, G. Tibbelin, R. Ladenstein, T. Lien, N.K. Birkeland, The 2.9A resolution crystal structure of malate dehydrogenase from Archaeoglobus fulgidus: mechanisms of oligomerisation and thermal stabilisation, Journal of molecular biology, 335 (2004) 343-356.
[21] D. Madern, X. Cai, M.S. Abrahamsen, G. Zhu, Evolution of Cryptosporidium parvum lactate dehydrogenase from malate dehydrogenase by a very recent event of gene duplication, Molecular biology and evolution, 21 (2004) 489-497.
[22] J.I. Boucher, J.R. Jacobowitz, B.C. Beckett, S. Classen, D.L. Theobald, An atomic-resolution view of neofunctionalization in the evolution of apicomplexan lactate dehydrogenases, eLife, 3 (2014).
[23] H. Schütte, W. Hummel, M.R. Kula, L-2-hydroxyisocaproate dehydrogenase—A new enzyme from Lactobacillus confusus for the stereospecific reduction of 2-ketocarboxylic acids, Appl Microbiol Biotechnol, 19 (1984) 167-176.
[24] G. Zhu, J.S. Keithly, Alpha-proteobacterial relationship of apicomplexan lactate and malate dehydrogenases, The Journal of eukaryotic microbiology, 49 (2002) 255-261.
[25] P.A. Steindel, E.H. Chen, J.D. Wirth, D.L. Theobald, Gradual neofunctionalization in the convergent evolution of trichomonad lactate and malate dehydrogenases, Protein Sci, 25 (2016) 1319-1331.
[26] G. Wu, A. Fiser, B. ter Kuile, A. Sali, M. Muller, Convergent evolution of *Trichomonas vaginalis* lactate dehydrogenase from malate dehydrogenase, Proceedings of the National Academy of Sciences of the United States of America, 96 (1999) 6285-6290.
[27] H.M. Wilks, K.W. Hart, R. Feeney, C.R. Dunn, H. Muirhead, W.N. Chia, D.A. Barstow, T. Atkinson, A.R. Clarke, J.J. Holbrook, A specific, highly active malate dehydrogenase by redesign of a lactate dehydrogenase framework, Science, 242 (1988) 1541-1544.
[28] F. Cendrin, J. Chroboczek, G. Zaccai, H. Eisenberg, M. Mevarech, Cloning, sequencing, and expression in Escherichia coli of the gene coding for malate dehydrogenase of the extremely halophilic archaebacterium Haloarcula marismortui, Biochemistry, 32 (1993) 4308-4313.
[29] W.E. Boernke, C.S. Millard, P.W. Stevens, S.N. Kakar, F.J. Stevens, M.I. Donnelly, Stringency of substrate specificity of Escherichia coli malate dehydrogenase, Archives of biochemistry and biophysics, 322 (1995) 43-52.
[30] T. Ohta, K. Yokota, T. Minowa, S. Iwata, Mechanism of allosteric transition of bacterial L-lactate dehydrogenase, Faraday discussions, (1992) 153-162.
[31] M.J. Reddish, H.L. Peng, H. Deng, K.S. Panwar, R. Callender, R.B. Dyer, Direct evidence of catalytic heterogeneity in lactate dehydrogenase by temperature jump infrared spectroscopy, J Phys Chem B, 118 (2014) 10854-10862.
[32] J.M. Gonzalez, R. Marti-Arbona, J.C.H. Chen, B. Broom-Peltz, C.J. Unkefer, Conformational changes on substrate binding revealed by structures of Methylobacterium extorquens malate dehydrogenase, Acta Crystallogr F Struct Biol Commun, 74 (2018) 610-616.
[33] M. Katava, M. Marchi, D. Madern, M. Sztucki, M. Maccarini, F. Sterpone, Temperature Unmasks Allosteric Propensity in a Thermophilic Malate Dehydrogenase via Dewetting and Collapse, J Phys Chem B, 124 (2020) 1001-1008.
[34] A.R. Clarke, D.B. Wigley, W.N. Chia, D. Barstow, T. Atkinson, J.J. Holbrook, Site-directed mutagenesis reveals role of mobile arginine residue in lactate dehydrogenase catalysis, Nature, 324 (1986) 699-702.
[35] A. Cortes, D.C. Emery, D.J. Halsall, R.M. Jackson, A.R. Clarke, J.J. Holbrook, Charge balance in the alpha-hydroxyacid dehydrogenase vacuole: an acid test, Protein Sci, 1 (1992) 892-901.
[36] T.J. Nobbs, A. Cortes, J.L. Gelpi, J.J. Holbrook, T. Atkinson, M.D. Scawen, D.J. Nicholls, Contribution of a buried aspartate residue towards the catalytic efficiency and structural stability of Bacillus stearothermophilus lactate dehydrogenase, Biochem J, 300 (Pt 2) (1994) 491-499.
[37] W. Eventoff, M.G. Rossmann, S.S. Taylor, H.J. Torff, H. Meyer, W. Keil, H.H. Kiltz, Structural adaptations of lactate dehydrogenase isozymes, Proceedings of the National Academy of Sciences of the United States of America, 74 (1977) 2677-2681.
[38] A.D. Chapman, A. Cortes, T.R. Dafforn, A.R. Clarke, R.L. Brady, Structural basis of substrate specificity in malate dehydrogenases: crystal structure of a ternary complex of porcine cytoplasmic

954 malate dehydrogenase, alpha-ketomalonate and tetrahydoNAD, Journal of molecular biology, 285
955 (1999) 703-712.
956 [39] V.J. Winter, A. Cameron, R. Tranter, R.B. Sessions, R.L. Brady, Crystal structure of Plasmodium
957 berghei lactate dehydrogenase indicates the unique structural differences of these enzymes are
958 shared across the Plasmodium genus, Mol Biochem Parasitol, 131 (2003) 1-10.
959 [40] S. Lunev, S. Butzloff, A.R. Romero, M. Linzke, F.A. Batista, K.A. Meissner, I.B. Muller, A. Adawy,
960 C. Wrenger, M.R. Groves, Oligomeric interfaces as a tool in drug discovery: Specific interference with
961 activity of malate dehydrogenase of Plasmodium falciparum in vitro, PloS one, 13 (2018) e0195011.
962 [41] S.R. Eddy, Accelerated Profile HMM Searches, PLoS computational biology, 7 (2011) e1002195.
963 [42] S. El-Gebali, J. Mistry, A. Bateman, S.R. Eddy, A. Luciani, S.C. Potter, M. Qureshi, L.J.
964 Richardson, G.A. Salazar, A. Smart, E.L.L. Sonnhammer, L. Hirsh, L. Paladin, D. Piovesan, S.C.E.
965 Tosatto, R.D. Finn, The Pfam protein families database in 2019, Nucleic acids research, 47 (2019)
966 D427-D432.
967 [43] K. Katoh, D.M. Standley, MAFFT multiple sequence alignment software version 7: improvements
968 in performance and usability, Molecular biology and evolution, 30 (2013) 772-780.
969 [44] M.N. Price, P.S. Dehal, A.P. Arkin, FastTree 2--approximately maximum-likelihood trees for large
970 alignments, PloS one, 5 (2010) e9490.
971 [45] S.Q. Le, O. Gascuel, An improved general amino acid replacement matrix, Molecular biology and
972 evolution, 25 (2008) 1307-1320.
973 [46] A. Criscuolo, S. Gribaldo, BMGE (Block Mapping and Gathering with Entropy): a new software for
974 selection of phylogenetic informative regions from multiple sequence alignments, BMC evolutionary
975 biology, 10 (2010) 210.
976 [47] L.T. Nguyen, H.A. Schmidt, A. von Haeseler, B.Q. Minh, IQ-TREE: a fast and effective stochastic
977 algorithm for estimating maximum-likelihood phylogenies, Molecular biology and evolution, 32 (2015)
978 268-274.
979 [48] S. Kalyaanamoorthy, B.Q. Minh, T.K.F. Wong, A. von Haeseler, L.S. Jermiin, ModelFinder: fast
980 model selection for accurate phylogenetic estimates, Nature methods, 14 (2017) 587-589.
981 [49] I. Letunic, P. Bork, Interactive Tree Of Life (iTOL) v4: recent updates and new developments,
982 Nucleic acids research, 47 (2019) W256-W259.
983 [50] T. Metsalu, J. Vilo, ClustVis: a web tool for visualizing clustering of multivariate data using
984 Principal Component Analysis and heatmap, Nucleic acids research, 43 (2015) W566-570.
985 [51] P. Schuck, Size-distribution analysis of macromolecules by sedimentation velocity
986 ultracentrifugation and lamm equation modeling, Biophys J, 78 (2000) 1606-1619.
987 [52] C.A. Brautigam, Calculations and Publication-Quality Illustrations for Analytical Ultracentrifugation
988 Data, Methods in enzymology, 562 (2015) 109-133.
989 [53] A. Le Roy, K. Wang, B. Schaack, P. Schuck, C. Breyton, C. Ebel, AUC and Small-Angle
990 Scattering for Membrane Proteins, Methods in enzymology, 562 (2015) 257-286.
991 [54] J.B. Dacks, M.C. Field, R. Buick, L. Eme, S. Gribaldo, A.J. Roger, C. Brochier-Armanet, D.P.
992 Devos, The changing view of eukaryogenesis - fossils, cells, lineages and how they all come together,
993 J Cell Sci, 129 (2016) 3695-3703.
994 [55] B.I. Lee, C. Chang, S.J. Cho, S.H. Eom, K.K. Kim, Y.G. Yu, S.W. Suh, Crystal structure of the
995 MJ0490 gene product of the hyperthermophilic archaebacterium Methanococcus jannaschii, a novel
996 member of the lactate/malate family of dehydrogenases, Journal of molecular biology, 307 (2001)
997 1351-1362.
998 [56] K. Niefind, H.J. Hecht, D. Schomburg, Crystal structure of L-2-hydroxyisocaproate dehydrogenase
999 from Lactobacillus confusus at 2.2 A resolution. An example of strong asymmetry between subunits,
1000 Journal of molecular biology, 251 (1995) 256-281.
1001 [57] D. Some, H. Amartely, A. Tsadok, M. Lebendiker, Characterization of Proteins by Size-Exclusion
1002 Chromatography Coupled to Multi-Angle Light Scattering (SEC-MALS), J Vis Exp, (2019).
1003 [58] L.J. Yennaco, Y. Hu, J.F. Holden, Characterization of malate dehydrogenase from the
1004 hyperthermophilic archaeon Pyrobaculum islandicum, Extremophiles : life under extreme conditions,
1005 11 (2007) 741-746.
1006 [59] A.K. Rolstad, E. Howland, R. Sirevag, Malate dehydrogenase from the thermophilic green
1007 bacterium Chloroflexus aurantiacus: purification, molecular weight, amino acid composition, and
1008 partial amino acid sequence, Journal of bacteriology, 170 (1988) 2947-2953.
1009 [60] C. Charnock, U.H. Refseth, R. Sirevag, Malate dehydrogenase from Chlorobium vibrioforme,
1010 Chlorobium tepidum, and Heliobacterium gestii: purification, characterization, and investigation of
1011 dinucleotide binding by dehydrogenases by use of empirical methods of protein sequence analysis,
1012 Journal of bacteriology, 174 (1992) 1307-1313.

[61] T. Oikawa, N. Yamamoto, K. Shimoke, S. Uesato, T. Ikeuchi, T. Fujioka, Purification, characterization, and overexpression of psychrophilic and thermolabile malate dehydrogenase of a novel antarctic psychrotolerant, Flavobacterium frigidimaris KUC-1, Biosci Biotechnol Biochem, 69 (2005) 2146-2154.
[62] D. Madern, The putative L-lactate dehydrogenase from Methanococcus jannaschii is an NADPH-dependent L-malate dehydrogenase, Molecular microbiology, 37 (2000) 1515-1520.
[63] H. Thompson, A. Tersteegen, R.K. Thauer, R. Hedderich, Two malate dehydrogenases in Methanobacterium thermoautotrophicum, Archives of microbiology, 170 (1998) 38-42.
[64] M. Nishiyama, J.J. Birktoft, T. Beppu, Alteration of coenzyme specificity of malate dehydrogenase from Thermus flavus by site-directed mutagenesis, The Journal of biological chemistry, 268 (1993) 4656-4660.
[65] I.K. Feil, H.P. Lerch, D. Schomburg, Deletion variants of L-hydroxyisocaproate dehydrogenase. Probing substrate specificity, European journal of biochemistry / FEBS, 223 (1994) 857-863.
[66] Y. Masukagami, K.A. Tivendale, G.F. Browning, F.M. Sansom, Analysis of the Mycoplasma bovis lactate dehydrogenase reveals typical enzymatic activity despite the presence of an atypical catalytic site motif, Microbiology (Reading), 164 (2018) 186-193.
[67] J.D. Evans, S.A. Martin, Cloning of the L-lactate dehydrogenase gene from the ruminal bacterium Selenomonas ruminantium HD4, Curr Microbiol, 44 (2002) 155-160.
[68] B.K. Ho, E.A. Coutsias, C. Seok, K.A. Dill, The flexibility in the proline ring couples to the protein backbone, Protein Sci, 14 (2005) 1011-1018.
[69] N. Coquelle, R. Talon, D.H. Juers, E. Girard, R. Kahn, D. Madern, Gradual adaptive changes of a protein facing high salt concentrations, Journal of molecular biology, 404 (2010) 493-505.
[70] R. Steuer, A.N. Nesi, A.R. Fernie, T. Gross, B. Blasius, J. Selbig, From structure to dynamics of metabolic pathways: application to the plant mitochondrial TCA cycle, Bioinformatics, 23 (2007) 1378-1385.
[71] H. Innan, F. Kondrashov, The evolution of gene duplications: classifying and distinguishing between models, Nat Rev Genet, 11 (2010) 97-108.
[72] S. Ohno, Evolution by gene duplication, Springer –Verlag, New-York, 1970.
[73] B. Binay, R.B. Sessions, N.G. Karaguler, A double mutant of highly purified Geobacillus stearothermophilus lactate dehydrogenase recognises l-mandelic acid as a substrate, Enzyme Microb Technol, 52 (2013) 393-399.
[74] D. Bur, T. Clarke, J.D. Friesen, M. Gold, K.W. Hart, J.J. Holbrook, J.B. Jones, M.A. Luyten, H.M. Wilks, On the effect on specificity of Thr246----Gly mutation in L-lactate dehydrogenase of Bacillus sterothermophilus, Biochemical and biophysical research communications, 161 (1989) 59-63.
[75] T. Dams, R. Ostendorp, M. Ott, K. Rutkat, R. Jaenicke, Tetrameric and octameric lactate dehydrogenase from the hyperthermophilic bacterium Thermotoga maritima. Structure and stability of the two active forms, European journal of biochemistry / FEBS, 240 (1996) 274-279.
[76] L.C. James, D.S. Tawfik, Conformational diversity and protein evolution--a 60-year-old hypothesis revisited, Trends in biochemical sciences, 28 (2003) 361-368.
[77] A. Wellner, M. Raitses Gurevich, D.S. Tawfik, Mechanisms of protein sequence divergence and incompatibility, PLoS genetics, 9 (2013) e1003665.

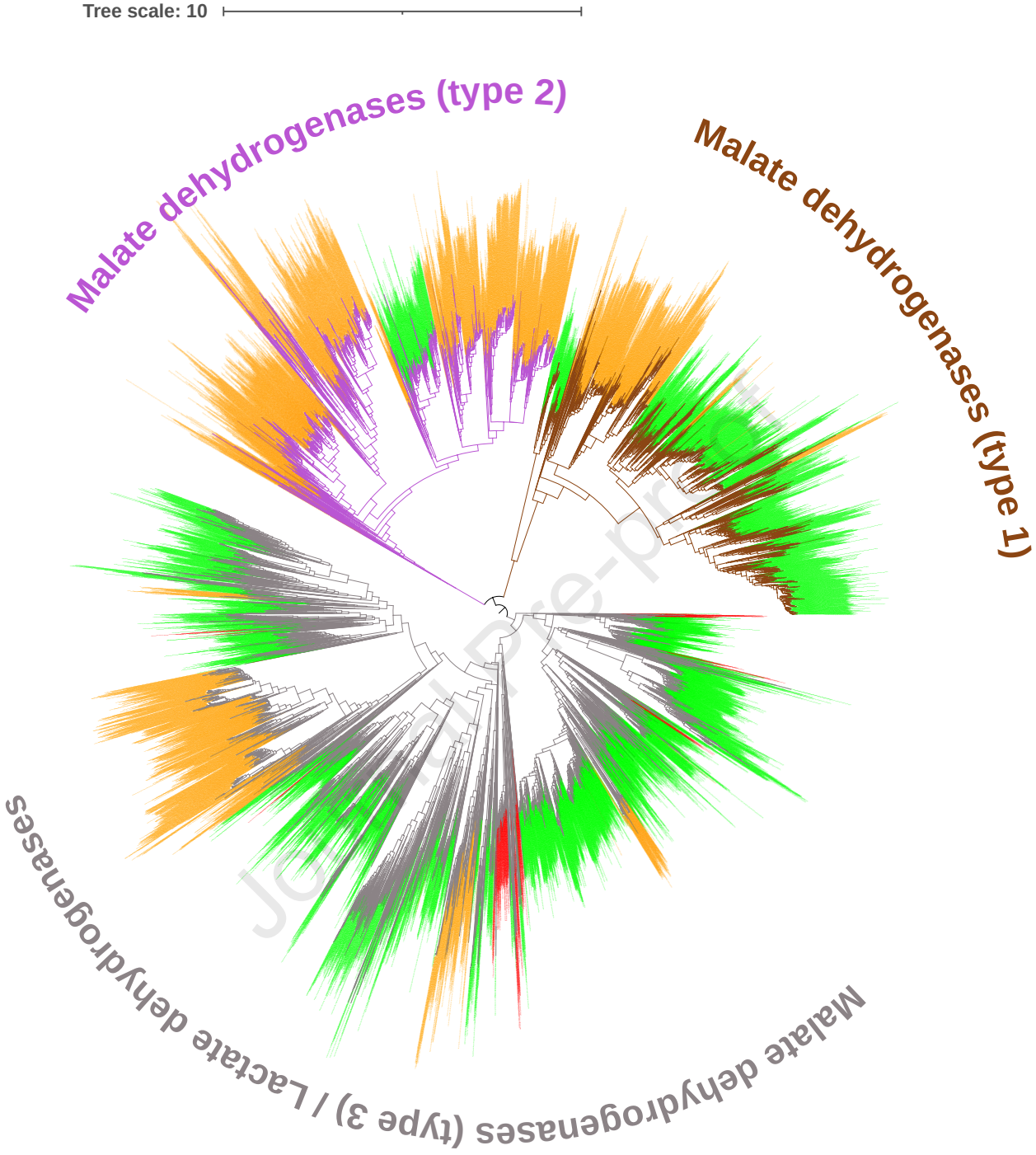

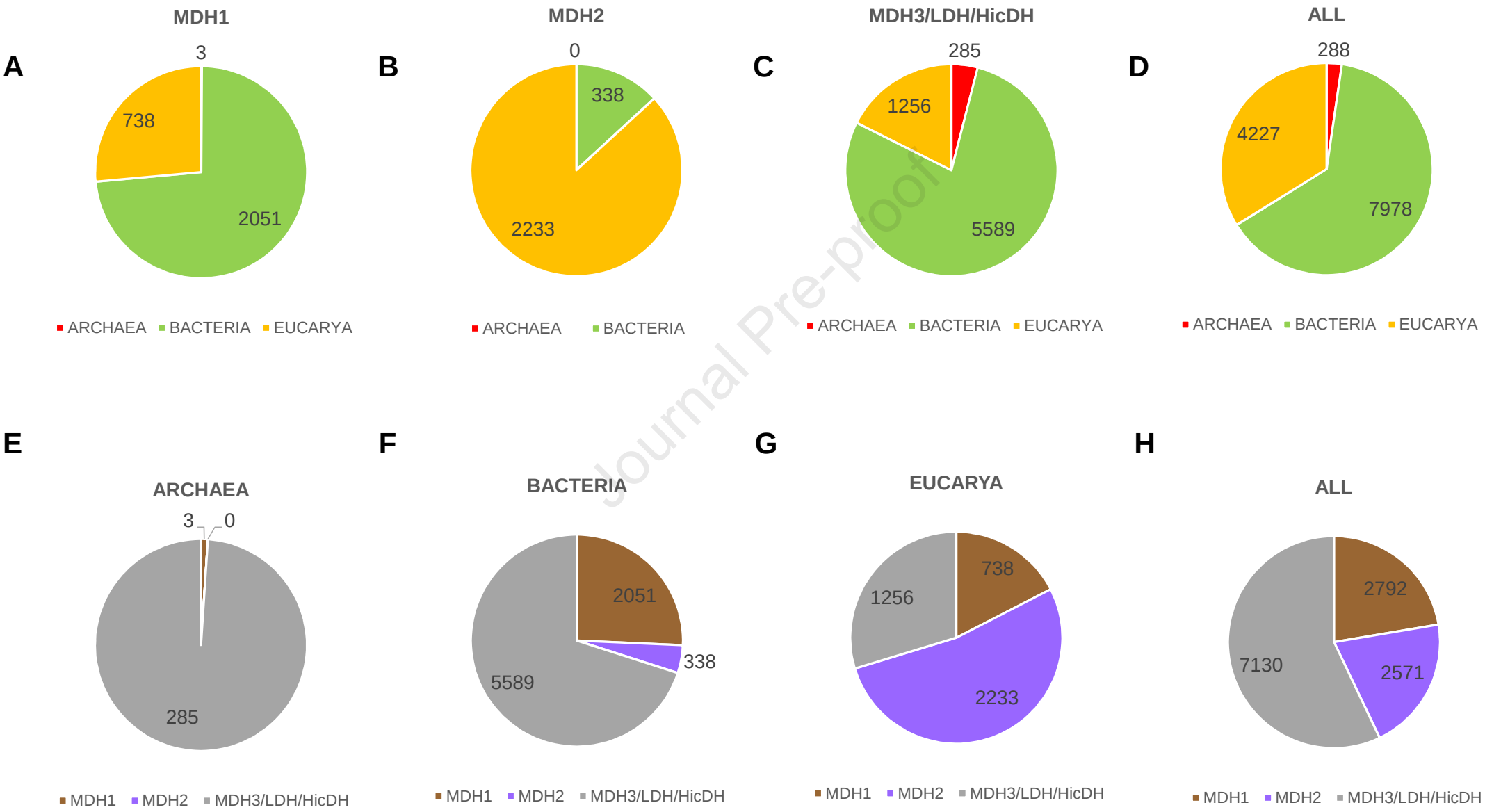

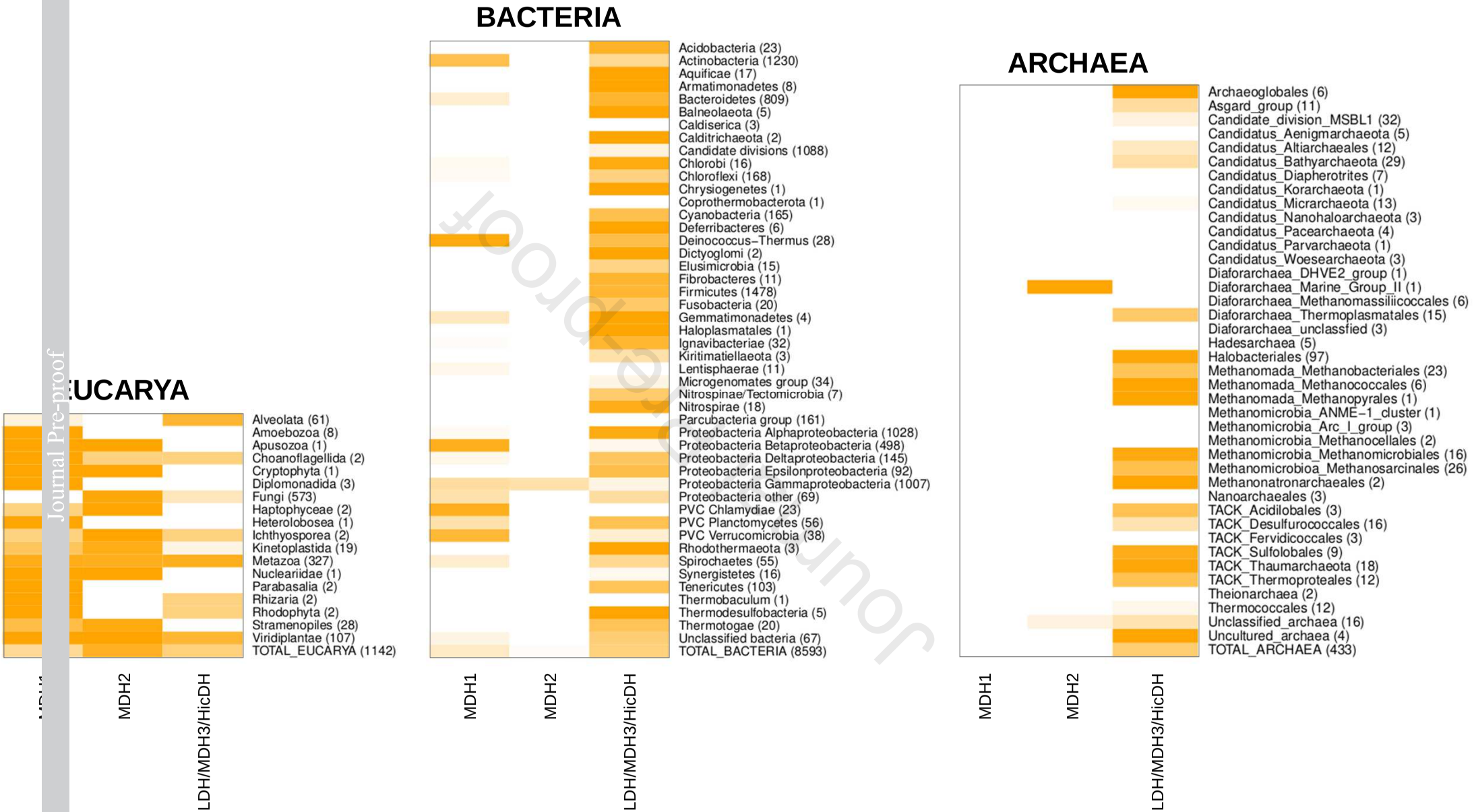

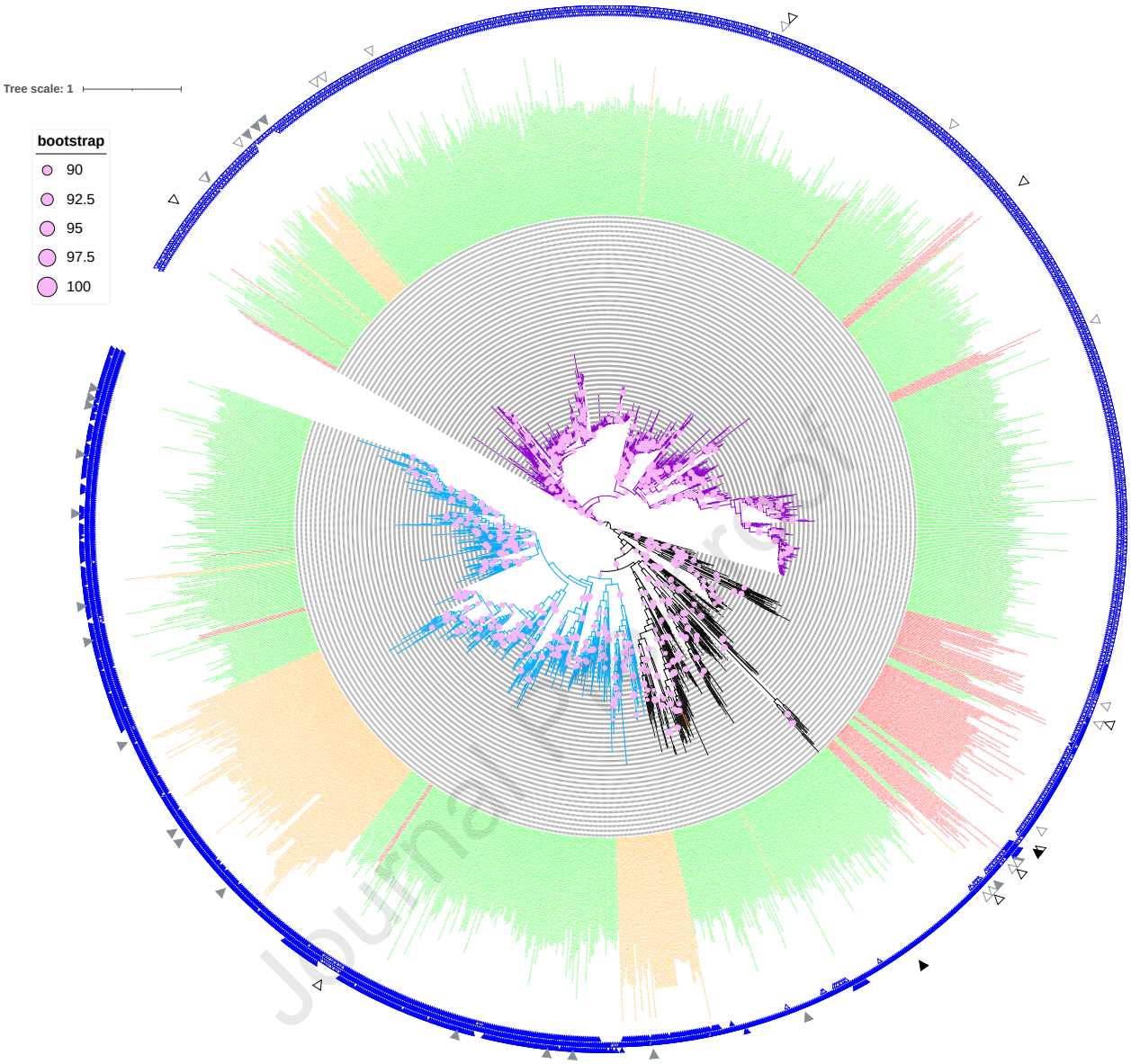

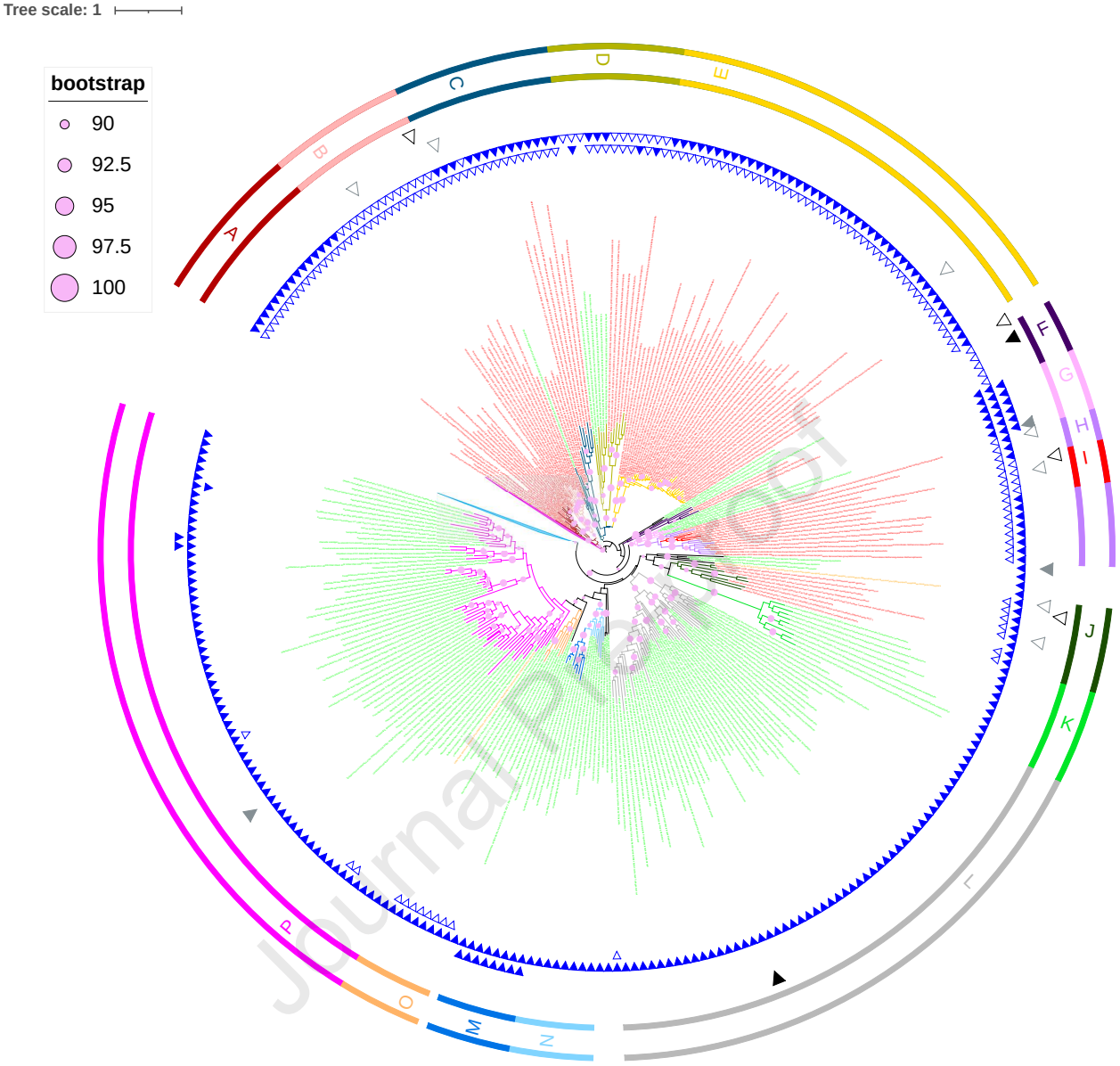

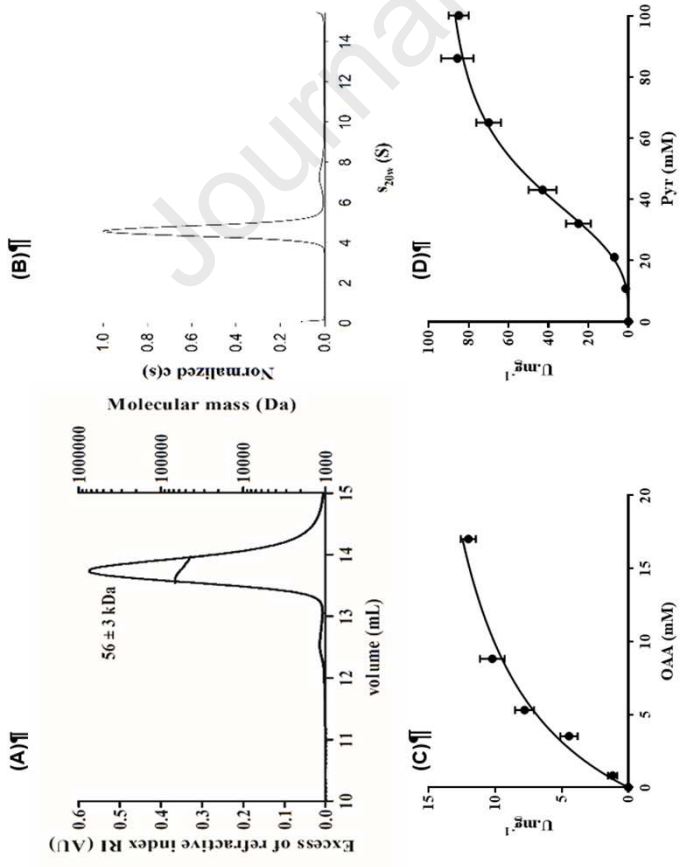

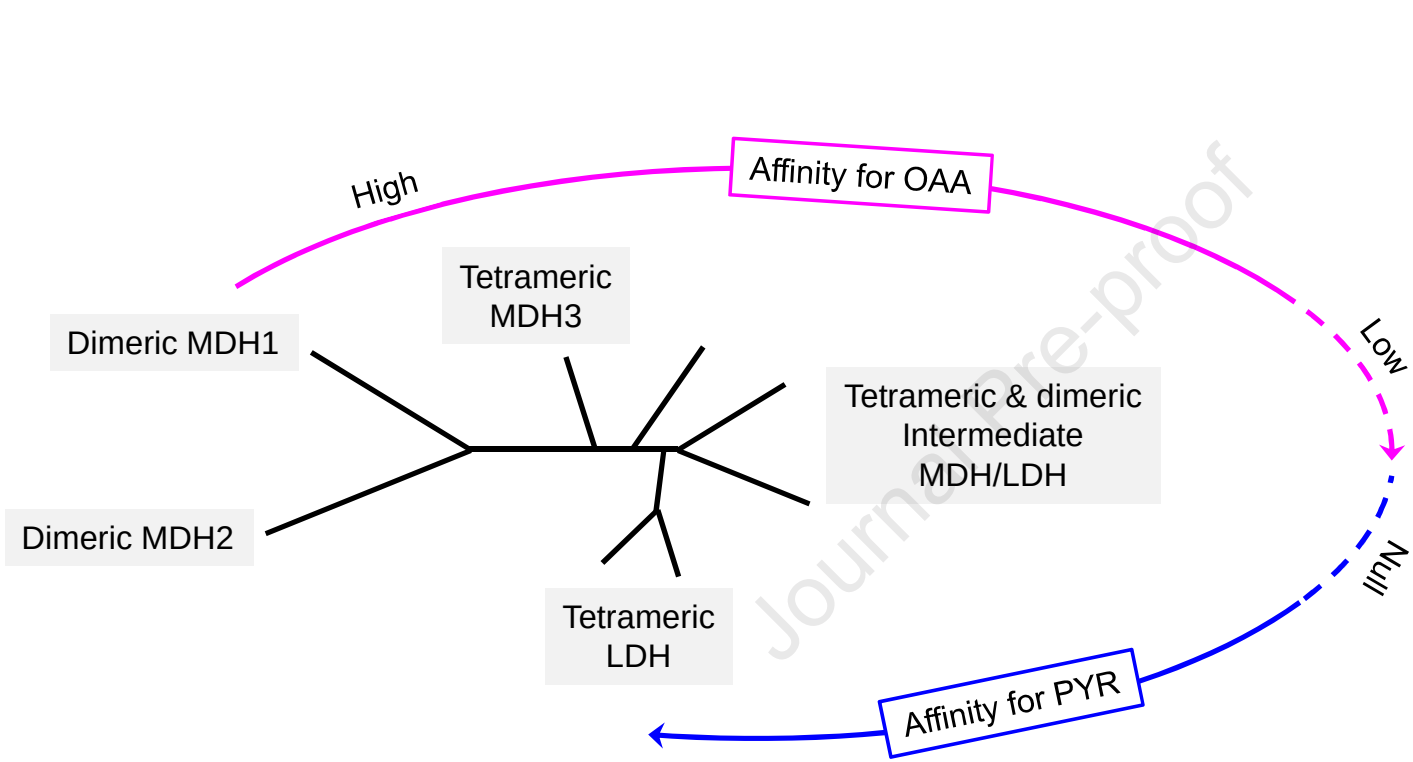

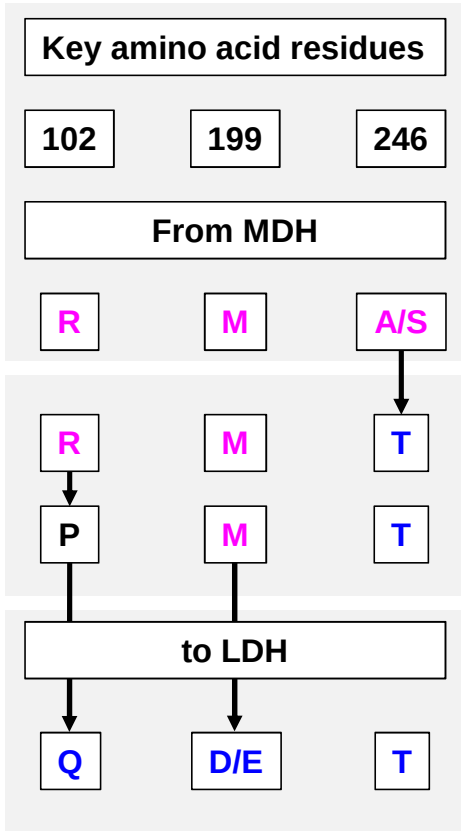

Highlights

Phylogenetic analyses disentangle the relationships between malate dehydrogenases and lactate dehydrogenases.

The study reveals an intermediate group of enzymes that reflects an early and step-wise functional divergence between malate dehydrogenases and lactate dehydrogenases.

Neofunctionalization and subfunctionalization contribute to evolution of malate dehydrogenases and lactate dehydrogenases.

The work suggests that present-day enzymes such as in *Tolumonas auensis* are descendant of an ancient group of enzymes in which allostery evolved.

Declarations of interest: none